Luo *et al. Energy Mater* 2024;4:400036
DOI: 10.20517/energymater.2023.119

Energy Materials

Review

Open Access

Check for updates

Recent development in addressing challenges and implementing strategies for manganese dioxide cathodes in aqueous zinc ion batteries

Chi Luo[1,#], Haoyun Lei[1,#], Yiyang Xiao[1], Xiaoxin Nie[2], Yuhang Li[2], Qian Wang[1], Wenlong Cai[1], Chunlong Dai[1,*], Meng Yao[1,*], Yun Zhang[1], Du Yuan[2,*]

[1]College of Materials Science and Engineering, Sichuan University, Chengdu 610065, Sichuan, China.
[2]College of Materials Science and Engineering, Changsha University of Science and Technology, Changsha 410004, Hunan, China.
[#]Authors contributed equally.

***Correspondence to:** Dr. Chunlong Dai, College of Materials Science and Engineering, Sichuan University, Yihuan Road 24, Chengdu 610065, Sichuan, China. E-mail: chunlongdai@scu.edu.cn; Dr. Meng Yao, College of Materials Science and Engineering, Sichuan University, Yihuan Road 24, Chengdu 610065, Sichuan, China. E-mail: yaomeng@scu.edu.cn; Dr. Du Yuan, College of Materials Science and Engineering, Changsha University of Science and Technology, 960, 2nd Section, Wanjiali RD (S), Changsha 410004, Hunan, China. E-mail: aduyuandu@outlook.com

How to cite this article: Luo C, Lei H, Xiao Y, Nie X, Li Y, Wang Q, Cai W, Dai C, Yao M, Zhang Y, Yuan D. Recent development in addressing challenges and implementing strategies for manganese dioxide cathodes in aqueous zinc ion batteries. *Energy Mater* 2024;4:400036. https://dx.doi.org/10.20517/energymater.2023.119

Received: 26 Dec 2023 **First Decision:** 7 Mar 2024 **Revised:** 19 Mar 2024 **Accepted:** 7 Apr 2024 **Published:** 18 Apr 2024

Academic Editor: Yuping Wu **Copy Editor:** Fangling Lan **Production Editor:** Fangling Lan

Abstract

Safety issues of energy storage devices in daily life are receiving growing attention, together with resources and environmental concerns. Aqueous zinc ion batteries (AZIBs) have emerged as promising alternatives for extensive energy storage due to their ultra-high capacity, safety, and eco-friendliness. Manganese-based compounds are key to the functioning of AZIBs as the cathode materials thanks to their high operating voltage, substantial charge storage capacity, and eco-friendly characteristics. Despite these advantages, the development of high-performance Mn-based cathodes still faces the critical challenges of structural instability, manganese dissolution, and the relatively low conductivity. Primarily, the charge storage mechanism of manganese-based AZIBs is complex and subject to debate. In view of the above, this review focuses on the mostly investigated MnO_2-based cathodes and comprehensively outlines the charge storage mechanisms of MnO_2-based AZIBs. Current optimization strategies are systematically summarized and discussed. At last, the perspectives on elucidating advancing MnO_2 cathodes are provided from the mechanistic, synthetic, and application-oriented aspects.

Keywords: Aqueous zinc ion battery, charge storage mechanism, manganese dioxide, optimization strategies

INTRODUCTION

As the non-renewable energy resources become gradually exhausted with their induced ecological and environmental pollution[1], the goals of carbon neutrality have immediately reached a global consensus. Finding renewable alternative energy sources has been the focus of attention and the key to solving the energy dilemma. Obviously, given the fluctuating nature of most renewable resources for power generation (e.g., wind, tide, solar, *etc.*), electrochemical energy storage devices have received widespread attention to provide a stable energy supply[2]. Many types of charge carriers, including potassium (K^+), sodium (Na^+), and lithium (Li^+), have been used in developing rechargeable battery technologies to date[3-8]. These developments have been made in systems such as organic electrolytes and aqueous electrolytes, providing a wider range of options for energy storage applications[9-15]. This diversity in charge carriers expands the potential for creating more efficient and tailored energy storage solutions.

Lithium-ion batteries are commonly employed in functioning electronic devices and electric automobiles in the present market[16]. However, their high cost, inadequate safety, and lack of resources are main drawbacks. These have long been recognized as the most common issues that lithium metal anodes encounter and have been considered obstacles to their commercialization[17]. In recent years, multivalent ion [e.g., magnesium (Mg^{2+}), calcium (Ca^{2+}), zinc (Zn^{2+}), *etc.*] battery systems have emerged as powerful alternatives with their inherited abundance[18-22]. In parallel, aqueous batteries revive with appreciable rechargeability[23], offering affordability, superior security, large theoretical capacity, *etc.* As the interdisciplinary representative of multi-valence ion and aqueous batteries, aqueous zinc ion batteries (AZIBs) are currently a hotspot in battery research. Zn is a potential anode material due to its high volumetric capacity of 5,855 mAh cm^{-3} and a substantial specific capacity of 820 mAh g^{-1}[24,25], with a relatively low redox potential of -0.76 V with reference to standard hydrogen electrode [Table 1][24-27]. Aqueous electrolytes are employed with higher safety, environmental friendliness, non-toxicity, and low volatility compared to non-aqueous batteries[28,29]. In addition, aqueous electrolytes possess superior ionic conductivity compared to organic electrolytes, enhancing the battery kinetics, including rate capability and charging/discharging capabilities[30]. A wide class of materials, e.g., Prussian blue analogs (PBAs), vanadium, nickel (Ni)-based, cobalt (Co)-based, and manganese (Mn)-based compounds, can be coupled with Zn anodes to construct AZIBs[31-39] [Figure 1A]. The electrochemical characteristics and reaction processes of the diverse AZIBs are outlined in Table 2 below. Among them, materials based on vanadium have drawn the most interest due to their strong electrochemical activity, which produces quick reaction kinetics, and their large theoretical capacity. Nevertheless, the energy storage capacity of AZIBs is constrained by the relatively modest voltage levels provided by vanadium-based materials[50]. As a typical metal-organic framework (MOF), analogs of Prussian blue can reach output voltages of approximately 1.6 volts, where the open pore structure provides a shorter and direct diffusion path for Zn^{2+} migration, promoting the rapid diffusion of Zn^{2+}. Ni-based cathodes are known for their stable energy delivery and extended lifespan, but their low electrical conductivity and irreversible phase changes pose significant challenges to their advancement[51]. Conversely, Co-based cathodes exhibit stable cycling ability and high theoretical capacity, but their practical application is limited by their poor electrical conductivity and inefficient capacity utilization[51]. The performance of AZIBs is restricted by the characteristics of cathode materials. The evolved crystallographic structure of cathode materials can lead to the deteriorated cycling stability. Most importantly, the zinc storage mechanism can be altered during the electrochemical process. As a result, investigating innovative cathode materials is essential for AZIB performance[52].

Mn, as an abundant transition metal, has divalent, trivalent, and trivalent states[53]. Among its oxide forms, manganese dioxide ($Mn(II)O_2$) has the most abundant crystallographic isomorphs. The fundamental structural unit of MnO_2 is the [MnO_6] octahedron. These units are linked together through angular or edge-

Table 1. A comparison of various capability parameters for lithium, sodium, potassium, zinc, magnesium, and calcium

Element	Li	Na	K	Zn	Mg	Ca
Relative atomic mass (g mol^{-1})	6.941	22.990	39.098	65.38	24.305	40.078
Ionic radius (Å)	0.76	1.02	1.38	0.74	0.72	1.00
Redox potential (V) *vs.* SHE	-3.04	-2.71	-2.92	-0.76	-2.37	-2.87
Melting point (°C)	180.5	97.8	63.5	419	650	842
Proportion	0.0017	2.36	2.09	0.0075	2.3	3.1

Table 2. A concise overview of the performance characteristics of various cathode materials in AZIBs

Cathode materials	Electrolyte component	Reaction mechanisms	Voltage (V)	Discharge capacity (mAh g^{-1})	References
V_2O_5	3 M $ZnSO_4$	Insertion/desertion mechanism	0.4-1.4	224 (100 mA g^{-1})	[40]
VS_2	1 M $ZnSO_4$	Insertion/desertion mechanism	0.4-1.4	190 (50 mA g^{-1})	[41]
CuHCF	1 M $ZnSO_4$	Insertion/desertion mechanism	0.2-1.2	56 (20 mA g^{-1})	[42]
ZnHCF	1 M $ZnSO_4$	Insertion/desertion mechanism	0.8-1.9	65.4 (60 mA g^{-1})	[43]
α-MnO_2	1 M $ZnSO_4$	Insertion/desertion mechanism	1.0-1.8	233 (83 mA g^{-1})	[44]
β-MnO_2	1 M $ZnSO_4$	Insertion/desertion mechanism	1.0-1.8	270 (100 mA g^{-1})	[45]
γ-MnO_2	1 M $ZnSO_4$	Insertion/desertion mechanism	1.0-1.8	285 (0.05 mA cm^{-1})	[46]
δ-MnO_2	1 M $ZnSO_4$	Insertion/desertion mechanism	1.0-2.0	269 (100 mA g^{-1})	[47]
Ni_4Co LDH@$Ag_{1.5}$NW	1 M KOH + 0.1 M $(CH_3COO)_2Zn$	Insertion/desertion mechanism	1.4-2.0	115.83 (100 mA g^{-1})	[48]
$ZnCo_2O_{4-x}$	2 M polyacrylamide (PAM)/$ZnSO_4$ hydrogel electrolyte		0.2-1.8	148.8 (50 mA g^{-1})	[49]

sharing connections to form various MnO_2 structures, such as one-dimensional (1D) tunnel structures (including α-MnO_2, β-MnO_2 and Todorokite manganite), two-dimensional (2D) layered structures, such as δ-MnO_2, and three-dimensional (3D) reticular structures (including the spinel-type μ-MnO_2)[54,55] [Figure 1B]. The unique properties of Mn-based materials make them a highly attractive choice for use as cathodes in AZIBs. However, there remain crucial problems that hinder their development: (1) during charging/discharging, Mn^{2+} undergoes an irreversible disproportionation reaction. The Jahn-Teller distortion of Mn^{2+} ions can cause the dissolution of manganese cathode materials over repeated charge-discharge cycles. Furthermore, the intercalation and deintercalation of protons can result in the by-product formation of layered double hydroxides on the MnO_2 surface, affecting the battery performance[56,57]; (2) Irreversible phase transitions can occur, leading to a significant reduction in the battery capacity over time. Zinc ions, with their relatively large ionic radius (0.76 Å) and potent electrostatic forces, are prone to forming strong bonds with oxygen atoms. This tendency results in substantial internal stress within the material during the cycling of charge and discharge. Consequently, this can trigger a breakdown of the material structure or induce a phase transformation[58,59]; and (3) Mn-based cathode materials typically show relatively poor electrical conductivity, which constrains the reaction kinetics[60]. These problems seriously affect the cell capacity, cycle stability, and Coulombic efficiency of AZIBs. To tackle these challenges, various strategies have been developed, focusing on preventing manganese dissolution, strengthening the structural integrity, and enhancing the electrical conductivity of the materials [Figure 1C].

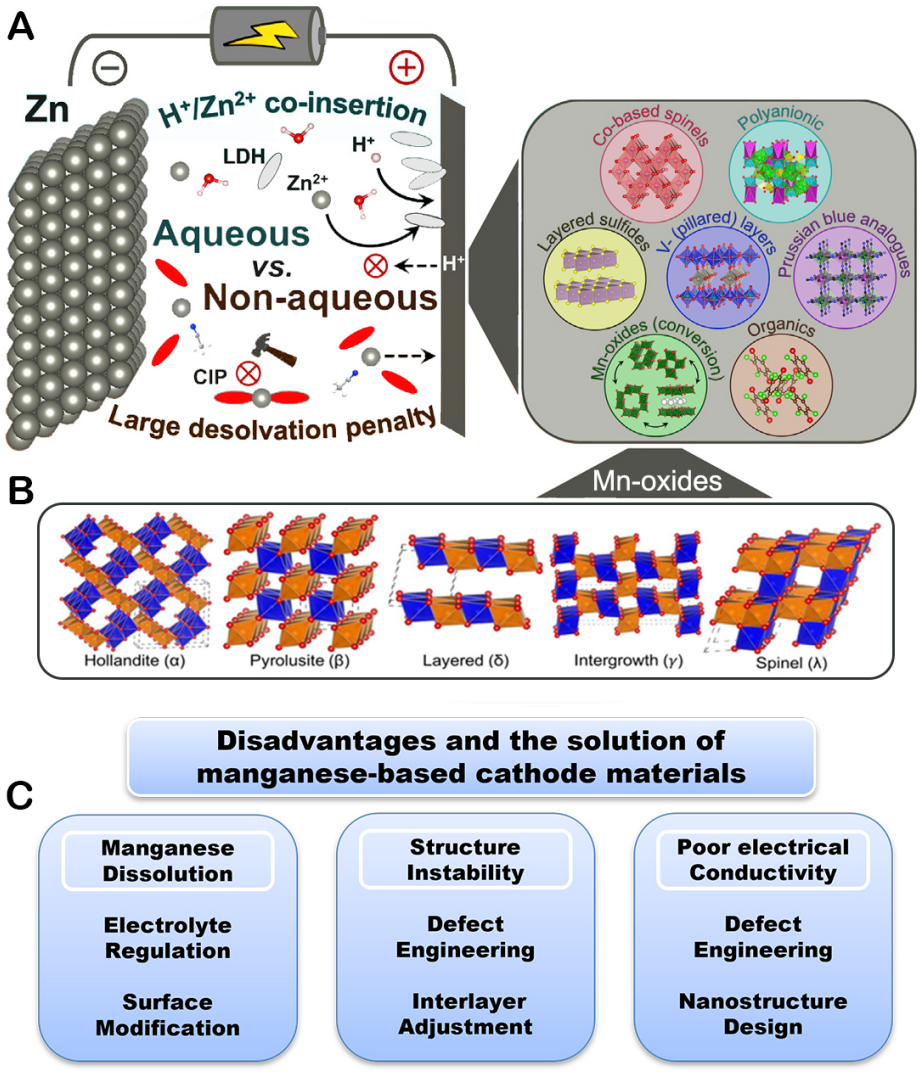

Figure 1. (A) Scheme of an aqueous zinc ion battery; (B) the polymorphs of MnO_2; (C) critical issues for the manganese-based cathode materials.

In light of the significance of Mn-based cathode materials, we have compiled this comprehensive review that concentrates on advancing and applying MnO_2-based materials in cutting-edge AZIBs. This review starts by examining charge storage mechanisms of AZIBs that utilize Mn-based cathode materials. More than dissolution-deposition mechanism, we update current understanding on the time-evolving pH effects on charge storage process and point out the necessity of correlating cathode structure and electrolyte design. Consequently, we focus on a more systematic discussion on the current methods for improving MnO_2-based cathode materials[61] from the perspectives of nanostructure design, interlayer adjustment, defect engineering, surface modification and electrolyte regulation. Finally, outlook and potential developments of Mn-based AZIBs are provided.

CHARGE STORAGE MECHANISMS FOR AZIBS

The diverse structural properties of cathode materials in AZIBs contribute to a more intricate and varied charge storage mechanism than the conventional rocking chair model observed in typical LIBs. This complexity arises from the interplay of ion insertion/extraction processes and structural transformations

within the cathode materials[62]. The differences in reaction mechanisms significantly influence the key performance of the battery. Additionally, research into the reaction mechanism of MnO_2-based cathodes is underway. Figure 2A gives a broad overview of the historical development of the reaction mechanism for MnO_2-based AZIBs. They evolved from the early alkaline MnO_2/Zn batteries. In 1986, Yamamoto pioneered the development of a prototype MnO_2/Zn battery by substituting the alkaline electrolyte with a neutral zinc sulfate solution, although the reaction mechanism was unclear at that time [Figure 2B][63]. Until 2011, Xu *et al.* presented the idea of AZIBs and disclosed the insertion/desertion process of Zn^{2+} on the MnO_2 cathode [Figure 2C][64]. With innovative material synthesis methods and characterization tools, Pan *et al.* proposed the mechanism of chemical transformation between α-MnO_2 and MnOOH [Figure 2C] in 2016[65]. In 2017, Sun *et al.* proposed a new mechanism, suggesting that both Zn^{2+} and H^+ ions could be involved in the insertion and extraction processes within the cathode material [Figure 2D][35]. In 2020, Zhu *et al.* enhanced the understanding of the reaction mechanism in zinc ion batteries (ZIBs) by exploring the precipitation-dissolution mechanism [Figure 2E][66]. The four main reaction mechanisms of the MnO_2 cathodes will be illustrated in detail.

Insertion/desertion mechanism

The insertion of Zn^{2+} is the most basic reaction mechanism of MnO_2 cathodes. Possessing an ionic radius of 0.74 Å, Zn^{2+} is easily deserted/inserted during the charging/discharging process, which exists in host materials with layer or tunnel structures. Since the inception of the MnO_2/Zn cell, the primary proposed mechanism for energy storage involved the reversible insertion and extraction of Zn^{2+}. Xu *et al.* contributed to this understanding by demonstrating that Zn^{2+} ions can indeed reversibly intercalate and deintercalate within the tunnel structure of α-MnO_2 when using electrolytes such as $ZnSO_4$ or $Zn(NO_3)_2$[64]. α-MnO_2 is converted to $ZnMn_2O_4$ after Zn^{2+} insertion. The reaction equations are given as:

$$\text{Cathode: } 2\alpha\text{-}MnO_2 + Zn^{2+} + 2e^- \leftrightarrow ZnMn_2O_4 \quad (1)$$

$$\text{Anode: } Zn \leftrightarrow Zn^{2+} + 2e^- \quad (2)$$

The crystal structure of α-MnO_2 is characterized by its large and settled tunnels, which are well-suited for accommodating guest cations, including Zn^{2+}, as depicted in Figure 3A. The tunnel structures are indeed pivotal for the reversible intercalation and deintercalation of Zn^{2+}, which are essential processes in the operation of ZIBs. Figure 3B provides a visual representation of the electrochemical activity of α-MnO_2 during the battery cycling. The presence of two distinct peaks near 1.3 and 1.7 V indicates the redox reactions occurring at the cathode during charging and discharging. The redox processes involving the insertion/extraction of Zn^{2+} ions from the α-MnO_2 structure are indicated by these peaks. The cycling behavior depicted in Figure 3C, where the material is evaluated in its pristine state, after Zn^{2+} ions are extracted at a potential of 1.7 V, and after Zn^{2+} ions are inserted at a potential of 1.3 V, confirms the reversible nature of these processes. Khamsanga and Alfaruqi highlight the advantages of using nanoscale δ-MnO_2, which has a shorter ion migration path than α-MnO_2. The characteristic of faster insertion and extraction of Zn^{2+} in δ-MnO_2 is indeed advantageous for enhancing the Zn^{2+} storage capacity. As shown in Figure 3D, the shorter ion migration path in δ-MnO_2 leads to a more efficient charge storage process, which is beneficial for the overall performance of ZIBs[67,68]. Note that this mechanism exists not only in MnO_2 but also in other cathodes in AZIBs, such as vanadium-based oxides[69], MnO[70], Mn_2O_3[66], organic compounds[71], and PBAs[42]. In 2012, Alfaruqi *et al.* showed that the MnO_x cathode in AZIB involves only the Zn^{2+} (de)intercalation reaction through MnO_x tunnels[46]. This mechanism implies that Mn disproportionation reactions result in metal ion dissolution, leading to accompanying pH variations during reactions. The observation of pH changes during electrode discharge cycling, ranging from approximately

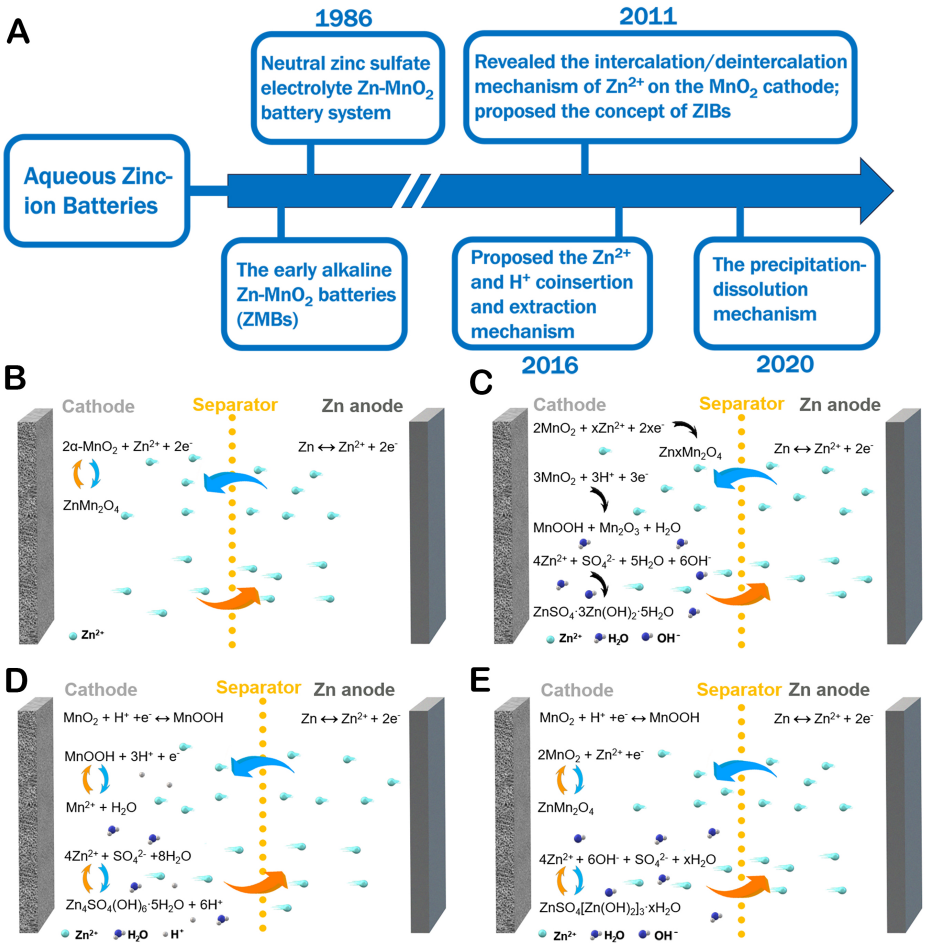

Figure 2. (A) Overview of the historical development of the reaction mechanism; (B) Zn^{2+} insertion/desertion mechanism; (C) Co-insertion/desertion mechanism; (D) Conversion reaction mechanism; (E) Dissolution-deposition reaction mechanism.

4.2 to more than 5.2, indicates the presence of a secondary or parasitic process distinct from the primary reaction. This suggests that the electrochemical behavior of MnO_x in ARZBs is more complex than initially anticipated.

Co-insertion/desertion mechanism

In cases where the cathode material features an open tunneling or layered structure, the electrochemical process can become more intricate than a simple Zn^{2+} ion insertion. In such instances, the reaction may also involve the participation of H^+[72] [Figure 4A]. Aqueous electrolytes in AZIBs contain a higher concentration of H^+ than non-aqueous electrolytes[55,73,74]. Using *in situ* X-ray diffraction (XRD) and *ex situ* transmission electron microscopy (TEM), Gao *et al.* confirmed the conjoined insertion and desertion of H^+ and Zn^{2+} in α-MnO_2[54]. H^+ insertion brings to the MnOOH (Mn^{4+} to Mn^{3+}). When H^+ is inserted at the MnO_2 cathode, the environment on the electrode surface becomes OH^- rich as the H^+ insertion, resulting in OH^- reacting with Zn^{2+} and SO_4^{2-} and forming zinc hydroxide sulfate ($[Zn(OH)_2]_3ZnSO_4{\cdot}5H_2O$) as a by-product in the electrolyte, as shown in the *in-situ* XRD spectra [Figure 4B]. During intercalation, where water-coordinated Zn^{2+} and Zn^{2+} ions are inserted into MnO_2, the resulting products are identified as $ZnMn_3O_7{\cdot}2H_2O$[75] and $ZnMn_2O_4$[76], as indicated by the XRD patterns in the corresponding charge/discharge states [Figure 4C]. This finding implies that the fluctuations in these peaks show a reversible Zn^{2+} insertion/desertion mechanism. The reaction equation for the -MnO_2/Zn cell is expressed as:

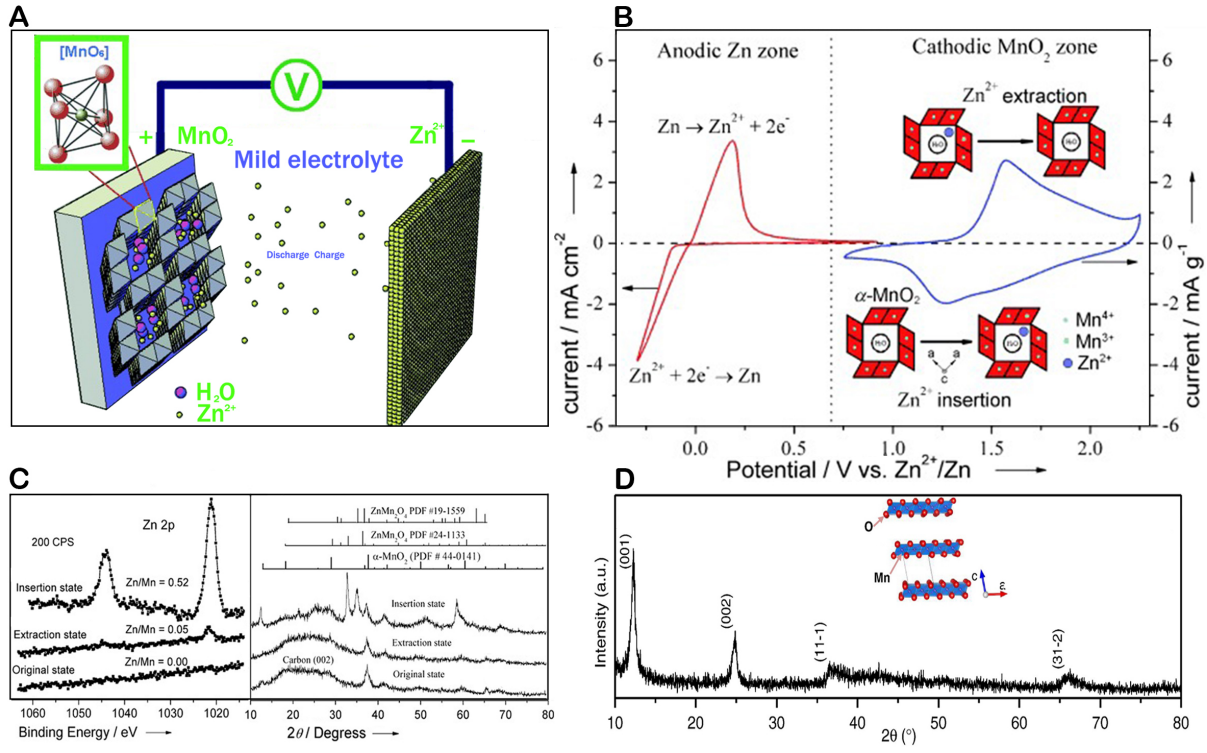

Figure 3. (A) Working mechanism of AZIB; (B) The graph depicts the anodic and cathodic reactions of the AZIB separately; (C) Zn 2p core level spectra and XRD patterns of cathodic crystalline α-MnO_2; This figure is reprinted (adapted) with permission from Xu *et al.* Copyright (2012) John/Wiley & Sons, Inc[64]. (D) XRD pattern of birnessite δ- MnO_2. This figure is reprinted (adapted) with permission from Alfaruqi *et al.* Copyright (2015) Elsevier Inc[68].

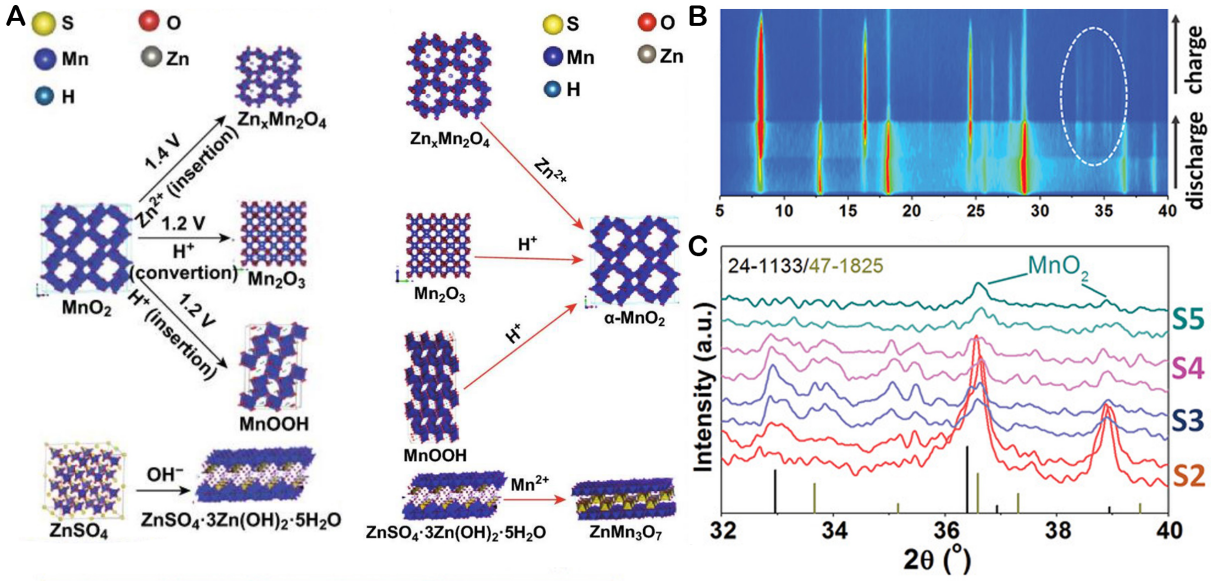

Figure 4. (A) Phase evolution of MnO_2; This figure is reprinted (adapted) with permission from Huang *et al.* Copyright (2019) Oahost[72]. (B) Phase evolution of cathode; (C) Contour graph of *in situ* XRD data. This figure is reprinted (adapted) with permission from Gao *et al.* Copyright (2020) Wiley VCH[54].

$$\text{Cathode: } 2MnO_2 + xZn^{2+} + 2xe^- \rightarrow Zn_xMn_2O_4 \quad (3)$$

$$MnO_2 + H^+ + e^- \rightarrow MnOOH \quad (4)$$

$$2MnO_2 + 2H^+ + 2e^- \rightarrow Mn_2O_3 + H_2O \quad (5)$$

$$4Zn^{2+} + SO_4^{2-} + 5H_2O + 6OH^- \rightarrow ZnSO_4 \cdot 3Zn(OH)_2 \cdot 5H_2O \quad (6)$$

$$\text{Anode: } Zn \rightarrow Zn^{2+} + 2e^- \quad (7)$$

Furthermore, Bi *et al.* demonstrated that $(Zn(OH)_2)_3(ZnSO_4)(H_2O)_4$ by-product exists on the cathode surface during H^+ insertion[77]. After the by-products were dissolved in a mild acid, Zn 2p signals were found using X-ray photoelectron spectroscopy (XPS). The Zn^{2+} and H^+ co-insertion/desertion is confirmed by the aforementioned results.

Conversion reaction mechanism

Other than the insertion/desertion type of charge storage mechanisms, Pan *et al.* proposed a chemical conversion reaction mechanism characterized by a chemical interaction between α-MnO_2 and MnOOH[65]. This mechanism is distinct from the traditional intercalation/deintercalation process and is based on the chemical transformation of the cathode material during discharging[65]. Upon complete discharge, protons originating from the water molecules in the electrolyte can react with α-MnO_2, producing MnOOH. During the discharge phase, hydroxide ions (OH^-) can engage in the reaction with $ZnSO_4$ and H_2O to generate a complex compound, $ZnSO_4[Zn(OH)_2]_3 \cdot xH_2O$ [Figure 5A], which renders the system electrically neutral. In addition to α-MnO_2, β-MnO_2 was also reported to exhibit this charge storage mechanism, and its cycling reaction route is shown in Figure 5B[78]. During the initial discharge phase, the transition from Mn^{3+} to Mn^{2+} occurs as protons react with β-MnO_2 to form MnOOH. The reaction process in the cathode involves the conversion and deposition of MnOOH and Mn^{2+} as ε-MnO_2 in the first charge. In later cycles, the MnOOH can be found, resulting from the reaction of the deposited MnO_2 with protons. During discharge, a portion of the MnOOH partially dissolves into Mn^{2+}, generating $Zn_4SO_4(OH)_6 \cdot 5H_2O$ (ZHS). During the charging process, the Mn^{2+} present in MnO_2 and ZHS is no longer detected. This cathode reaction process can be succinctly given as:

$$MnO_2 + H^+ + e^- \leftrightarrow MnOOH \quad (8)$$

$$MnOOH + 3H^+ + e^- \leftrightarrow Mn^{2+} + H_2O \quad (9)$$

$$4Zn^{2+} + SO_4^{2-} + 8H_2O \leftrightarrow Zn_4SO_4(OH)_6 \cdot 5H_2O + 6H^+ \quad (10)$$

The pH value shown in Figure 5C increases during discharging and decreases during the charge phase. This supports the involvement of H^+ in the electrode reaction process. In the chemical conversion reaction mechanism, new materials are formed, unlike the first two ion-inserted energy storage mechanisms. In this process, hydrogen ions are the only ions inserted/extracted into the cathode material, while Zn^{2+} is primarily converted to ZHS and does not participate directly in the charging/discharging reactions. The energy density and cycle life of batteries are influenced by the types and amounts of conversion-type cathodes and the category and structure of substrates[79]. Note that the crystal phase and electrolyte differences in manganese oxide necessitate a thorough and precise analysis of the reaction mechanism.

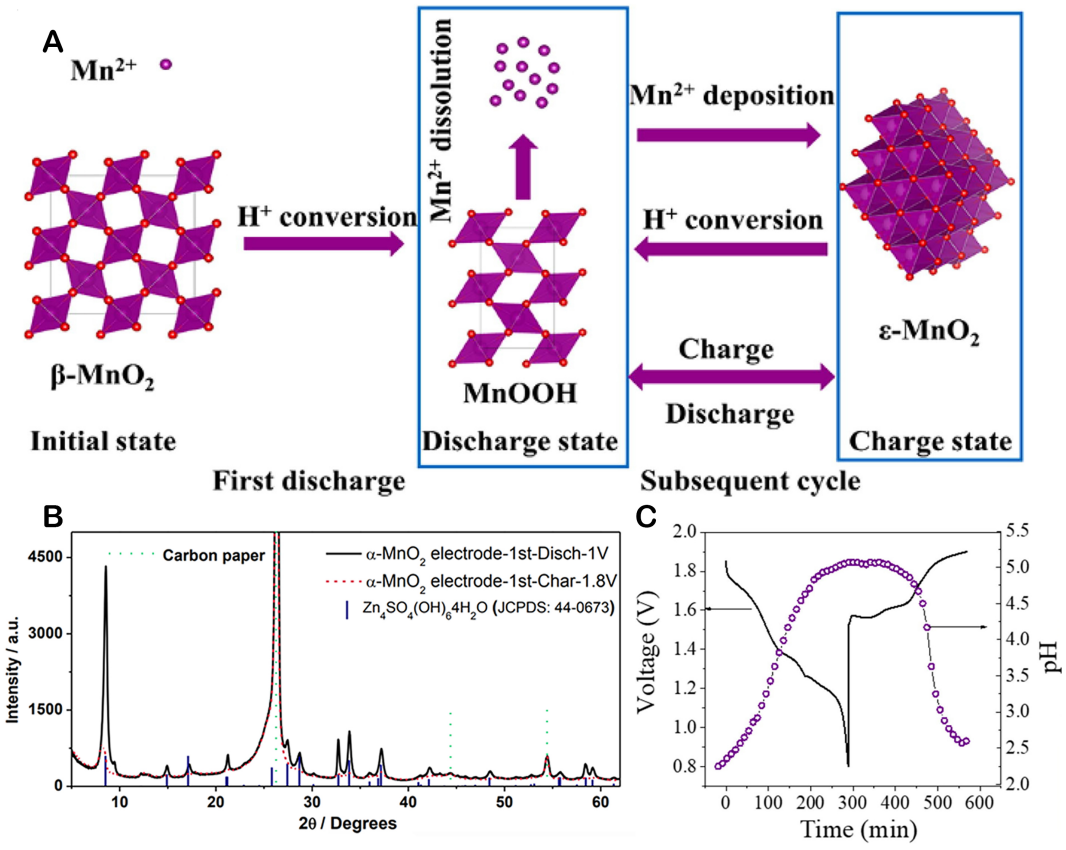

Figure 5. (A) The reaction path of β-MnO_2; (B) The XRD patterns of α-MnO_2; This figure is reprinted (adapted) with permission from Pan *et al.* Copyright (2016) Nature Research[65]. (C) *In situ* pH changes of β-MnO_2/Zn. This figure is reprinted (adapted) with permission from Liu *et al.* Copyright (2021) Elsevier[78].

Dissolution-deposition mechanism

The dissolution-deposition process involves the electrical charge transfer between the electrodes, propelled by an electrical potential gradient. This process occurs under both kinetic and thermodynamic constraints, and it allows for the reversible movement of charges between the deposited electrode materials, facilitating the transformation of electrodeposition products back into soluble forms[80]. Liang *et al.* designed a MnO_2/Zn battery based on the deposition-dissolution mechanism, with an electrolyte containing 0.3 mol/L $ZnSO_4$ and 0.3 mol/L $MnSO_4$[81]. The new full battery design operates at a voltage approximately 0.55 V higher than traditional MnO_2-based aqueous batteries, attributed to the reaction of the deposition-dissolution mechanism.

In 2020, Guo *et al.* found that the insertion/desertion of Zn^{2+} and H^+ occurred at the same time as the reaction, as illustrated in Figure 6A[82]. The discharge process of the first cycle with α-MnO_2 or δ-MnO_2 as the host material involves a series of reactions that produce Mn^{2+} and OH^- ions. These ions then react with the surrounding $ZnSO_4$ in the electrolyte to form ZHS, which consumes a significant amount of H_2O. The depletion of H_2O in the vicinity of MnO_2 suppresses the subsequent dissolution of MnO_2, increasing the Mn^{2+} content in the electrolyte and pH. On the other hand, the newly formed ZHS reacts with Mn^{2+} during the charge process of the first cycle to produce birnessite-MnO_2, which substitutes for the original MnO_2 as the host material. This dissolution-deposition mechanism is a key process that dominates the energy storage process and significantly contributes to the specific capacity of the battery. In subsequent cycles, this dissolution-deposition mechanism continues to recur, with birnessite-MnO_2 acting as the host material. The

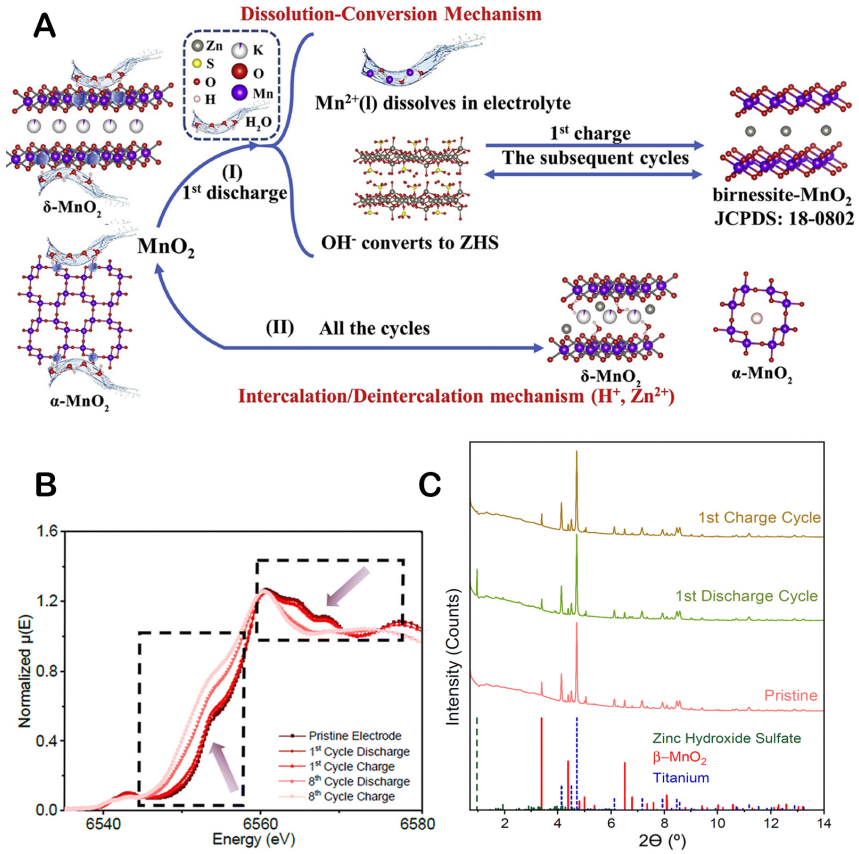

Figure 6. (A) Energy storage mechanism in MnO_2/Zn batteries. This figure is reprinted (adapted) with permission from Guo *et al.* Copyright (2020) Elsevier[82]. (B) Mn K-edge *ex situ* XAS; (C) Operando X-ray diffraction results. This figure is reprinted (adapted) with permission from Kankanallu *et al* Copyright (2023) RSC Publishing.[83].

intercalation/de-intercalation reaction of Zn^{2+} ions into and out of the MnO_2 structure is considered less critical in the overall energy storage process. In their study, Kankanallu *et al.* investigated the chemical, morphological, and structural alterations that occur in β-MnO_2 due to the dissolution-deposition process[83]. A multimodal approach was employed, integrating operando X-ray diffraction and absorption spectroscopy and X-ray microscopy. Figure 6B and C highlights that the main capacity during the first discharge cycle comes from the dissolution of MnO_2 into Mn^{2+} ions. In parallel, the deposition of ZHS takes place in close proximity to the dissolution site, forming a layered structure on the MnO_2 surface. Upon charging, two distinct Zn-Mn complex phases are deposited within the electrode. One is an amorphous phase that can be reversibly formed, while the other is a crystalline phase that is not reversible. Li *et al.* studied a redox chemical reaction involving MnO_2/Mn^{2+} and interfacial regulation[84]. The study observed that the discharge initially caused the dissolution of MnO_2 due to H^+ conversion, consequently increasing the pH value and Mn^{2+} concentration in the electrolyte. Following this, the formation of ZHS occurred, with the process being largely governed by intricate dissolution and deposition reactions. As the charging phase progressed, the concurrent deposition of Zn^{2+} and Mn^{2+} created a Zn-rich birnessite phase, $ZnxMn_3O_7$, while simultaneously causing the dissolution of ZHS. Subsequently, this was followed by the conversion of $Zn_xMn_3O_7$ to Mn_7O_{13} through Zn^{2+} desertion and Mn^{2+} deposition. In addition, there is a reverse phase transition where the simultaneous insertion of Zn^{2+} and H^+ ions induces the $Zn_xMn_3O_7$ dissolution, generating ZHS. Continued insertion of H^+ ions results in the further dissolution of $Zn_xMn_3O_7$ until the final formation of ZHS is achieved[84].

The proposal of the deposition-dissolution mechanism has laid the theoretical foundation for the next-generation MnO_2/Zn batteries. Unlike the ongoing debate over the dual- or single-electron transfer in conventional mildly acidic ARZBs, the Mn deposition-dissolution involves a dual electron transfer via the Mn^{2+}/Mn^{4+} redox reaction. Consequently, the theoretical capacity of MnO_2/Zn batteries has doubled, reaching a promising value of 616 mAh g^{-1}.

The charge storage mechanism of MnO_2-based AZIBs has been a subject of debate since its early development. While various reaction routes have been proposed, several critical factors continue to pose challenges. Understanding the charge storage mechanism of AZIBs is still ongoing, although it is established that the process is not merely a straightforward insertion/desertion mechanism. It is important to note that the exact function of Mn^{2+} additives in electrochemical processes, especially concerning intercalation and/or conversion reactions, is not yet fully understood. Researchers are still exploring how these additives influence the reaction mechanisms and the overall performance of the electrochemical systems. Further investigation is required to elucidate the specific effects of Mn^{2+} on the electrochemical behavior. Unlike the study conducted by Lee, which employed *in situ* pH analysis to investigate the correlation between electrolyte pH and the formation of ZBS [Figure 7A][85], there is limited comprehensive research on the structural and phase changes and the influence of pH during the charge and the discharge cycles of the MnO_2 positive electrode in AZIBs[72]. Also, the impact of Mn^{2+} additives on the fluctuations of pH and the precise function of ZBS remains ambiguous, mainly due to the variations in the concentrations of additives and salts employed in the reported configurations. Excess additives can hinder ZBS formation, which, however, can be significantly influenced by factors such as the changing electrolyte pH (according to the Nernst equation: $\Delta E = Ec - Ea = \left(E_c^\theta - E_a^\theta\right) + \frac{RT}{nF} ln(\frac{C_{H^+}^4}{C_{Mn^{2+}}})$. The reduction in H^+ concentration decreases the activation energy needed for Mn deposition. Increasing pH leads to the formation of a large amount of inert "dead Mn", causing capacity decay and the generation of electrolytic MnO_2 [Figure 7B][86,87]. The claim that MnOOH acts as an intermediate or final discharge product in the presence of Mn^{2+} additives, which would imply a proton conversion reaction, is indeed a subject of contention. Although this claim is supported by *ex situ* characterizations, where the presence of MnOOH has been detected, it has not been confirmed by *in situ* analyses, underscoring the need for further clarification.

The electrochemical performance of MnO_x cathodes in AZIBs is influenced by the crystallographic structure of the MnO_x polymorphs. Table 3 lists the various forms and crystal structures of MnO_2, highlighting the different tunnel structures important for ion insertion and extraction. Among the tunnel-type cathodes, such as α-MnO_2, β-MnO_2, todorokite-type MnO_2, and γ-MnO_2, are particularly noteworthy. Additionally, δ-MnO_2, λ-MnO_2, $ZnMn_2O_4$, and Mn_3O_4 have also been reported to show moderate performance in ARZBs. Despite numerous studies on the specific crystalline types of MnO_x in AZIBs, there is a gap in understanding the relationship between the crystal structure of MnO_x polymorphs and their corresponding performances[87,94], where few studies have been reported. The electrochemical performance of various manganese oxide polymorphs is known to decrease under specific electrochemical conditions, with the order of performance being α > δ > γ > λ > β[95]. It is anticipated that α- and γ-MnO_2 cathodes will exhibit capacity-driven reactions in Regions I and II. Furthermore, the charge storage mechanism for MnO_2 cathodes is dynamic throughout their lifespan, as shown in Figure 7C. The pH level of the electrolyte can induce progressive alterations in Region II, where the primary process is cathodic dissolution, influencing the associated capacity contribution. To validate these assumptions and fully understand the relations amidst crystal structure and electrochemical performance, comprehensive electrochemical analysis is required. This analysis would involve systematic studies that explore the effects of crystal structure, electrolyte composition, and electrochemical conditions on the performance of MnO_x cathodes in zinc batteries, which is critical for optimizing the materials and electrolytes for improved battery performance.

Table 3. Type and crystal structure of MnO_2

Type	Crystal structure or space group	Lattice constants/Å	Theoretical structures	References
α-MnO_2	Monoclinic A2/m	a = b = 9.93 c = 2.86	T2 × 2	[90]
β-MnO_2	Rutile structure P42/mnm	a = b = 4.41 c = 2.88	T1 × 1	[78]
β-MnO_2	Pbnm	a = 4.66 b = 2.94 c = 9.34	T1 × 2	[53]
γ-MnO_2	Ortho.	a = 9.61 b = 2.84 c = 4.42	T1 × 1 & 1 × 2	[91]
δ-MnO_2	Birnessite	a = b = 2.83 c = 14.31	L(m × ∞)	[92]
λ-MnO_2	Defect spinel structure	a = b = c = 8.09	N(m × n)	[93]
ε-MnO_2	Defective NiAs $P6_3/mmc$	a = b = 2.83 c = 4.46	T1 × 1 & 2 × 2	[53]

T: Tunnel; L: layer; N: net; (m × n): the count of [MnO_6] octahedra in the cross-sectional and longitudinal directions.

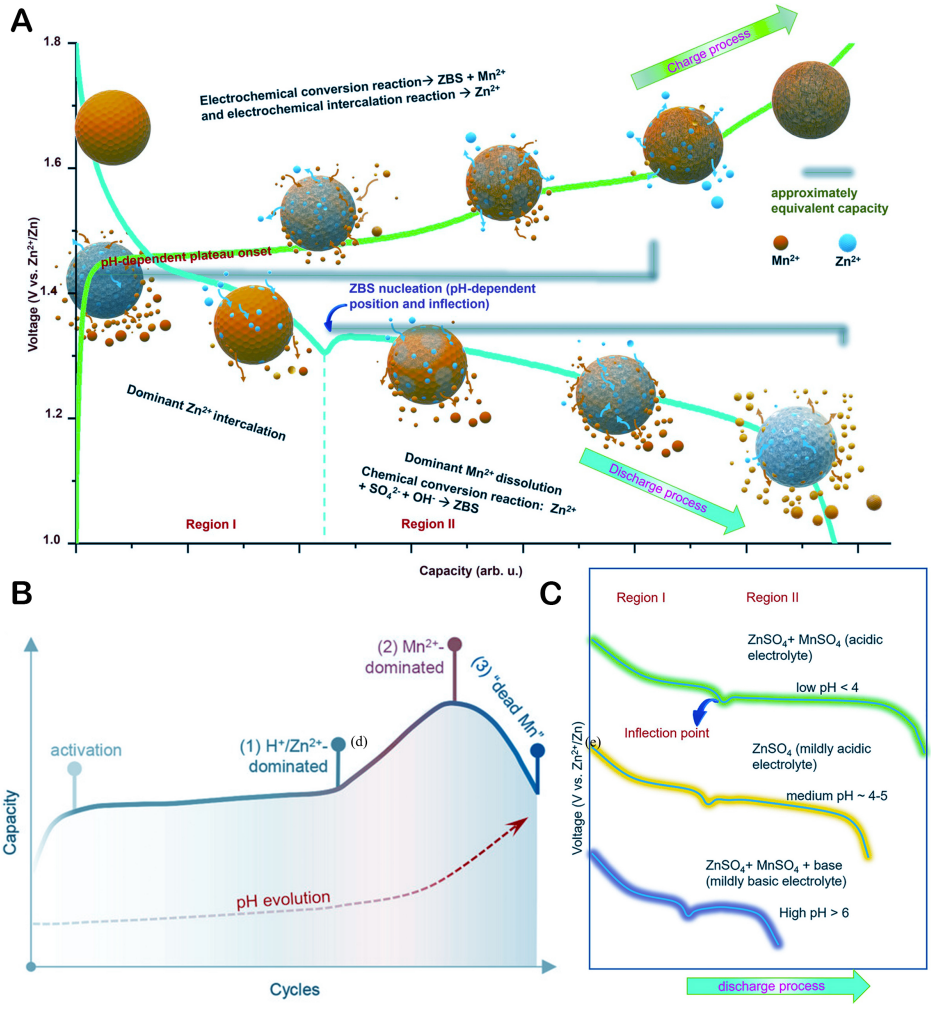

Figure 7. (A) Schematic representation of the proposed electrochemical reaction in a typical MnO_2/Zn aqueous battery. (B) The development of storage capacity and the mechanisms involved in energy storage during cycles that are influenced by variations in pH levels. This figure is reprinted (adapted) with permission from Yang *et al.* Copyright (2023) Wiley-VCH[88]. (C) Schematic galvanostatic discharge profiles. This figure is reprinted (adapted) with permission from Sambandam *et al.* Copyright (2022) Elsevier Inc[89].

THE STRATEGIES OF PERFORMANCE OPTIMIZATION FOR MNO_2-BASED CATHODE

Though being promising, MnO_2-based cathodes face critical challenges in AZIBs, among which the three most critical ones are: (a) Manganese dissolution: during the cycling process, the active substance in the electrode dissolves in the electrolyte through disproportionation reaction and produces irreversible side reaction products, which directly leads to the rapid decay of battery capacity; (b) Structural instability: all polymorphs of MnO_2 usually undergo structural transformation during repeated intercalation/decalcification of hydrated H^+/Zn^{2+} ions, severe structural disruption, and volumetric changes, which leads to capacity degradation in AZIBs; and (c) Poor electrical conductivity: manganese oxides usually have poor electrical conductivity limiting the rate of electron transfer. Consequently, Mn-based cathode materials of AZIBs present drawbacks in terms of cycling and rate capability. Facing above challenges, several strategies have been employed on MnO_2 cathodes, including nanostructure design, interlayer spacing, and defect engineering, surface modification, and electrolyte regulation.

Nanostructure design

The advanced capability of nanostructured electrode materials to improve the storage and discharge of foreign ions is achieved by reducing the diffusion distance for electron and ion transfer, thereby enhancing the diffusion dynamics. Such enhancement is ascribed to (a) the increased surface area-to-volume ratio, which affords more active sites to electrochemical reactions; and (b) the unique structural characteristics in the nanoscale for an electrode. Nanostructure can be classified into four categories: (a) zero-dimensional (0D); (b) 1D; (c) 2D; and (d) hierarchical structure.

Consequently, due to their distinct surface and structural properties, nanomaterials of varying diameters display a range of performances[96]. Nanomaterials (not only MnO_2 nanomaterials) with 0D structures, such as those with particle sizes below 100 nm, offer a short pathway for ion diffusion and a broad interface with the electrolyte[97,98]. This enables them to offer distinct advantages; for instance, Wei *et al.* showed the creation of α-MnO_2 with a surface area of 208 $m^2\ g^{-1}$ and a substantial initial discharge capacity of 234 mA h g^{-1}[47]. This was achieved using spherical nanoparticles and cylindrical nanorods, which were synthesized through co-precipitation. Additionally, 1D structured materials not only facilitate rapid ion diffuseness in the radial direction but also promote swift electron transport along the 1D axis[99]. Alfaruqi *et al.* proved this advantage by creating MnO_2 nanorods with a huge specific surface area of 153 m^2/g and an amazing first discharge specific capacity of 323 mA h/g using a straightforward solvent-free manufacturing technique[100]. That highlighted the potential of 1D structured materials in battery applications[100]. These unique structural characteristics provide distinct advantages over 0D structured nanoparticles. Furthermore, 2D nanomaterials, such as layered MnO_2 nanosheets, boast unique advantages over their 0D and 1D counterparts thanks to their expanded interlayer spacing, high surface-to-volume ratio, and atomic-level thickness. These features provide 2D nanomaterials with a greater number of active sites and remarkable mechanical flexibility, which has been evidenced in the work of Choi[101], who synthesized layered MnO_2 nanosheets delivering a large discharge capacity of 350 mA h/g. These findings highlight the diverse performance and potential of different dimensional nanomaterials in various applications.

In addition to nanostructured MnO_2, nanocomposite was prepared to boost the performance for MnO_2 cathodes. Li *et al.* demonstrated the synthesis of a 3D core-shell structured layered MnO_2 on N-doped carbon nanowires for use as a cathode material [Figure 8A and B][102]. Despite the similar shapes and two pairs of distinct redox peaks observed in the cyclic voltammetry (CV) curves of both samples [Figure 8C], the δ-MnO_2 nanosheets on N-doped carbon nanowires (MnO_2@NC) cathode demonstrated a superior peak current density, which is a sign of enhanced electrochemical storage capacity. This phenomenon was further

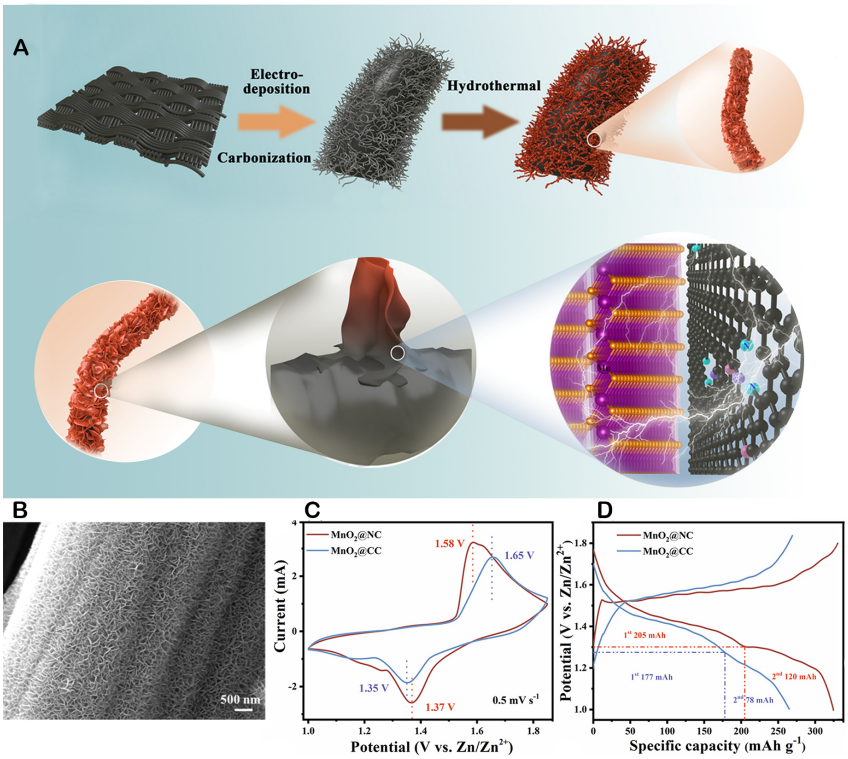

Figure 8. (A) Schematic representation of preparation process for MnO_2@NC electrode; (B) SEM images of MnO_2@CC; (C) CV curves at 0.5 mV s^{-1}; (D) GCD curves at 0.1 A g^{-1}[102]. This figure is reprinted (adapted) with permission from Li *et al.* Copyright (2022) Wiley[102].

confirmed by the higher capacity of the MnO_2@NC cathode compared to the MnO_2 nanosheets grown on bare carbon nanofibers (MnO_2@CC) cathode, as shown in Figure 8D. The superior electrochemical performance of the MnO_2@NC cathode is attributed to the enhanced conductivity of the N-doped carbon nanowires. MnO_2@NC cathode material exhibits a higher capacitance than MnO_2@CC cathode material (325 mAh g^{-1} at 100 mA g^{-1}). Moreover, MnO_2@NC demonstrates outstanding rate performance and stable cycling, maintaining around 95% of its original capacity after 2,500 cycles at a current density of 2A/g. Zhang *et al.* studied the integration of MnO_2 nanosheets onto a skeleton of N-doped porous carbon nanosheets to enhance the reactivity and electrical conductivity of the cathode material[103]. Through a comprehensive investigation into the mechanisms responsible for the improved performance of the MnO_2 composite electrode in batteries, they found that the N-doped carbon played a pivotal role in lowering the valence state of Mn^{4+} ions within the MnO_2 structure. This reduction in valence state was instrumental in mitigating the electrostatic repulsion between Zn^{2+}/H^+ during the embedding process, thus facilitating a higher degree of cation insertion and accelerating ion migration within the electrode.

Interlayer adjustment

The impact of unstable electrode material structure on AZIBs during reaction can be improved by adjusting the interlayer spacing [Figure 9A][101]. Nam *et al.* explored the effect of structural water content on the capability of layered MnO_2 (cw-MnO_2). Their research indicated a direct correlation between the water content in cw-MnO_2 and the battery capacity [Figure 9B][101]. Specifically, they found that cw-MnO_2 with an optimal water molecule content of 0.94 exhibited superior capacity, reaching up to 350 mA h g^{-1}. This finding was further supported by the data presented in Figure 9C-E, which clearly demonstrated the enhanced performance of the cw-MnO_2 with the ideal amount of structural water. This finding indicates

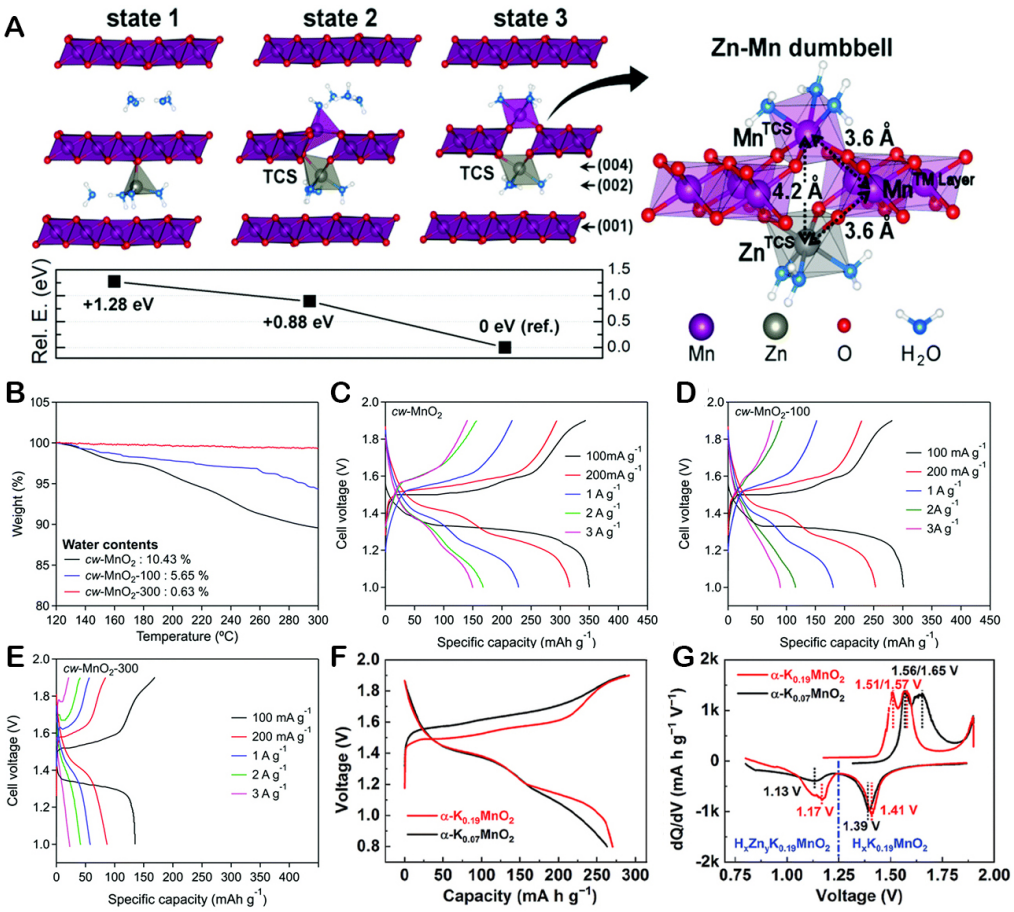

Figure 9. (A) Zn^{2+}-Intercalated structures and relative energies; (B) TGA profiles of pristine. Discharge-charge voltage profiles at various current densities for (C) pristine cw-MnO, (D) cw-MnO_2-100, and (E) cw-MnO_2-300; This figure is reprinted (adapted) with permission from Nam *et al.* Copyright (2019) RSC Publishing[101]. (F) Discharge-charge curves for the second cycle (G) differential discharge-charge capacity curves. This figure is reprinted (adapted) with permission from Liu *et al.* Copyright (2019) Royal Society of Chemistry[104].

that suitable water content and interlamellar spacing can help achieve a satisfactory cycle performance by preventing manganese dissolution and preserving the integrity of the electrode structure during cycling. However, the optimal quantity of structural water remains uncertain. Determining how the layer spacing of Mn-based materials and their electrochemical performance relate to the quantity of structural water is crucial. The presence of structural water increases interlayer spacing, shielding electrostatic interactions and thereby facilitating foreign cation diffusion and stabilizing the host structure. However, an elevated content of structural water promotes rapid Zn^{2+} diffusion, which compromises structural stability and adversely affects the electrochemical performance.

Furthermore, as a pillar to support the structure, guest species can be pre-intercalated into the cathode material of a tunnel or layered construction. Liu *et al.* delved into the effects of pre-intercalated K^+ ions on the electrochemical properties of tunnel-structured MnO_2-graded nanotubes, denoted as α-$K_{0.19}MnO_2$[104]. For comparison, α-$K_{0.07}MnO_2$ nanotubes were prepared. The investigation demonstrated that the shape and crystal structure of α-$K_{0.07}MnO_2$ nanotubes did not change following the removal of K^+. Although the discharging/charging plateaus of both materials were comparable in slope [Figure 9F], the α-$K_{0.19}MnO_2$ cathode showed a lower overpotential. Furthermore, as shown in Figure 9G, it exhibited a higher capacity,

reaching 270 mAh g^{-1}. Furthermore, the redox potential of the α-$K_{0.19}MnO_2$ cathode material is lower during insertion/extraction of Zn^{2+} and H^+ ions. This implies that the reversible insertion/extraction of H^+ and Zn^{2+} into the MnO_2 is facilitated by the presence of K^+ ions.

Besides, nucleating agents can be added in the preparation stage of MnO_2 to improve the layer spacing. Hong *et al.* reduced the energy barrier of MnO_2 crystal growth, nucleation and refinement by adding a polyethylene glycol (PEG) nucleating agent in the preparation stage of MnO_2, which made PEG-regulated δ-MnO_2 (PR-δ-MnO_2) have smaller average grain diameter, higher specific surface area and water-rich interlayer[105]. Compared to the original δ-MnO_2, PR-δ-MnO_2 has a greater capacity (295 mAh g^{-1}), better magnification, and increased cycle stability.

Defect engineering

Nanostructure defect

MnO_2-type crystalline forms are prone to substantial phase transitions and dissolution of Mn during cycling, forming structural collapses that lead to poor long-term cycling performance. Moreover, the advancement of Mn-based cathodes in energy storage is hindered by the challenge of sluggish reaction kinetics, which results from the intense electrostatic interactions between Zn^{2+} ions and the substrate material. Amorphous manganese dioxide has attracted a lot of attention because of its rich structural flaws and short-range atomic groupings as a solution to this problem. These defects are beneficial in secondary batteries as they can act as reversible ion storage sites, thereby improving ion diffusion kinetics and enhancing the overall capacity of the battery[106-109]. The incorporation of oxygen vacancies within the amorphous MnO_2 structure is particularly noteworthy. These vacancies can significantly accelerate charge storage kinetics, allowing for more efficient lithium-ion insertion and deintercalation processes. Moreover, the oxygen-deficient structure of amorphous MnO_2 has been shown to contribute to remarkable electrochemical stability, which is crucial for the longevity and reliability of energy storage devices[110]. On the flip side, the inherently isotropic nature of an amorphous structure can play a pivotal role in mitigating the strain that arises from volume changes during the cycling process. This characteristic is particularly beneficial as it can help minimize the degradation of the electrode material over time[111,112]. Cai *et al.* explored an amorphous manganese dioxide (A-MnO_2-δ) electrode material based on abundant structural defects and intrinsic anisotropy, which possesses structural defects that can act as reversible ionic storage sites, enhance ion diffusion kinetics, and increase battery capacity[113]. This amorphous manganese oxide avoids structural collapse during cycling, which enables high-speed zinc ion diffusion kinetics as a cathode for high-speed and stable aqueous rechargeable ZIBs. Its structural flaws may improve battery capacity and ion diffusion kinetics by serving as reversible ion storage sites. Furthermore, the material amorphous structure exhibits an inherently isotropic behavior that may aid in relieving the pressures brought on by volume variations and lessen the electrode material deterioration. A high specific capacity of 301 mAh g^{-1} at 100 mA g^{-1} and 78% capacity retention rate after 1,000 cycles are provided by A-MnO_2-δ.

Heteroatom doping

Defect introduction can involve using specific methods to create vacancies in the positive electrode material, thereby inducing structural defects. It can also be achieved by doping impurity atoms into the positive electrode material to create heterogeneous atomic defects or by replacing specific elements in Mn-based composite materials to enhance the electrochemical potential of the positive electrode material.

Liang *et al.* have investigated a novel approach to enhance the electrochemical performance of electrodes by altering their surface characteristics and the associated reaction kinetics[114]. They found that incorporating graphite nanosheets (GNS) with high hydrophobicity and minimal oxygen defects can effectively impede

the rate-limiting step of Mn^{2+} adsorption. This manipulation of the surface properties creates free-standing MnO_2 electrodes that exhibit remarkable stability, particularly during high depth of discharge (DOD) cycling and when subjected to multiple charge-discharge cycles. Post-cycling analysis of these electrodes revealed that the occurrence of undesired side reactions was significantly delayed and reduced. This finding challenges the conventional belief that extending the effective cycle life of a cell could be achieved solely by inhibiting the *in situ* electrodeposition of MnO_2. The electrodes developed through this strategy demonstrate a significantly extended cycling life, surpassing 600 cycles, while preserving the high C-rate stability that is characteristic of α-MnO_2. The outstanding performance of the electrodes validates the kinetic inhibition strategy proposed by the researchers. This strategy not only improves the cycling stability of MnO_2/Zn batteries but also offers a new avenue for developing rechargeable batteries with long cycle lives. Hu *et al.* improved the electrochemical performance by depositing highly conductive Co_9S_8 on Ni foams (NF) to form a layered core-shell structure, as shown in Figure 10A, which provided a greater number of electrochemically active sites[115]. This method essentially involves first synthesizing MnO_2 on NF and then heat treating it at 400 °C to form bean sprout-like MnO_2, as shown in Figure 10B. Next, a simple hydrothermal method was used to uniformly grow MnO_2@Co_3O_4 nanowires on MnO_2/NF. Subsequently, an amino exchange reaction was carried out on Co_3O_4/MnO_2/NF to form a MnO_2@Co_3O_4 core-shell structure, and finally, MnO_2@Co_9S_8 was synthesized through a vulcanization reaction. The number of electrochemically reactive active sites and conductivity of the electrode material were increased by coating the MnO_2 arrays with highly conductive Co_9S_8. This enables the MnO_2@Co_9S_8/NF electrode to have a high specific capacitance that is 3.4 and 10.1 times greater than that of the Co_3O_4@MnO_2 and pure MnO_2 electrodes, respectively. It achieves an impressive area capacitance of 1,540 mC cm^{-2} and an energy density of 346.5 mWh cm^{-2}. Additionally, it maintains a capacity retention of 97.5% after 36,000 cycles, showcasing its excellent stability. By achieving high efficiency, stability, and long-life operation, these methods provide new concepts and solutions for AZIBs. This is anticipated to encourage the advancement and use of ZIB technology with more environmentally beneficial outcomes.

Surface modification

Surface coatings offer a range of functions and properties that make them essential in various industrial applications. One primary function is to protect against corrosion, wear, oxidation, and pollution. This safeguards the underlying materials and substrates, prolonging their lifespan. In this regard, surface coating provides an effective method for optimizing manganese dioxide cathode materials for AZIBs. It can enhance the stability of manganese dioxide. By forming a protective film on the surface of MnO_2, it can prevent unnecessary reactions with the external environment. This protective film can block the entry of oxygen, moisture, and other harmful substances. Also, surface coating methods can effectively inhibit the dissolution of the cathode material and shield the electrostatic interaction between guest ions[91,116].

Carbon materials are frequently used as coatings for MnO_2 cathode materials in batteries. The cycle stability of the electrode is improved by this coating process, which is especially efficient in declining the dissolution of manganese ions from the cathode. A straightforward and economical technique has been devised by Islam *et al.* to generate α-MnO_2@C or carbon-coated nanoparticles, which function very well as cathodes in AZIBs[117]. The synthesis process uses maleic acid ($C_4H_4O_4$) as the carbon source to create a gel, which is then subjected to annealing at a relatively low temperature of 270 °C[117]. TEM analysis confirmed the presence of a uniform carbon network interspersed among the α-MnO_2 nanoparticles. This carbon coating not only enhanced the structural integrity of the nanoparticles but also contributed to improved electrochemical performance. The α-MnO_2@C composite exhibited a remarkable initial discharge capacity of 272 mAh g^{-1} at a current density of 66 mA g^{-1}, which is a significant improvement over the pristine α-MnO_2, which had a discharge capacity of 213 mAh g^{-1} under the same conditions. Moreover, the α-MnO_2@C composite demonstrated superior cycling stability compared to the original α-MnO_2. This

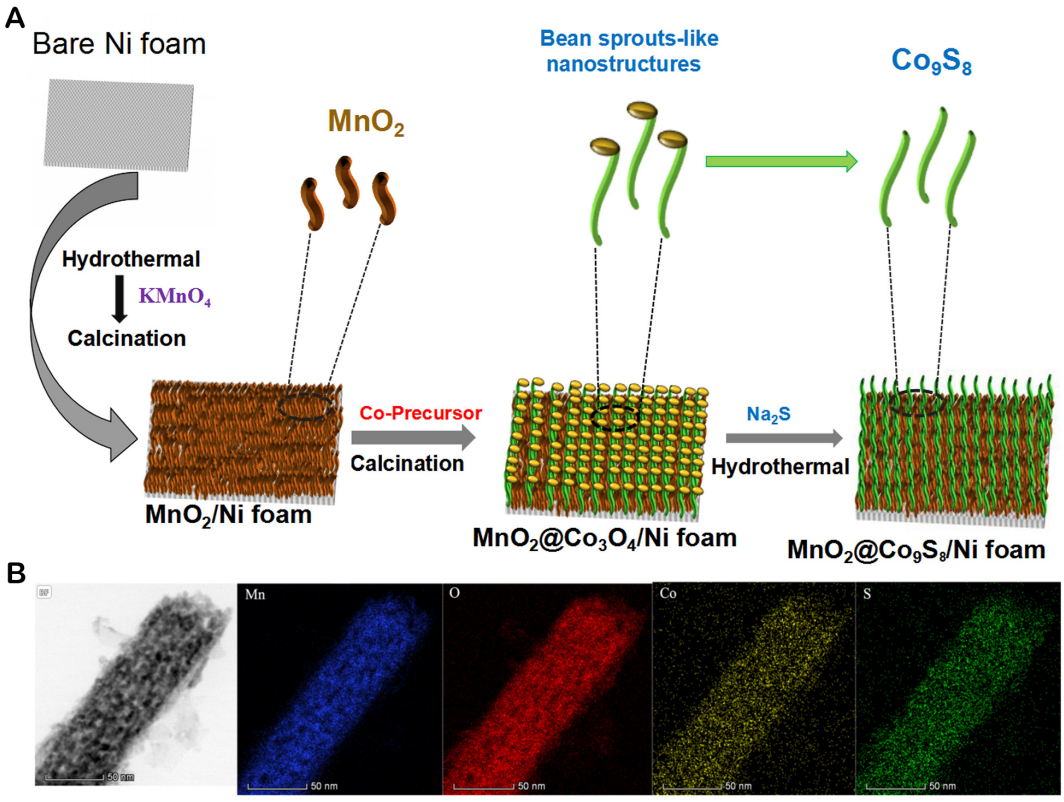

Figure 10. (A) Schematic representation of preparation process for MnO_2@Co_9S_8/NF; (B) Transmission mapping images of the core-shell structured MnO_2@Co_9S_8/NF. This figure is reprinted (adapted) with permission from Hu *et al.* Copyright (2021) Pergamon[115].

enhanced stability is likely due to the protective effect of the carbon coating, which mitigates the dissolution of manganese ions during cycling, thereby preserving the integrity of the cathode material and maintaining its capacity over extended charge-discharge cycles[117]. In the CV curves presented in Figure 11A, a comparison between the pristine α-MnO_2 electrode and the α-MnO_2@C electrode reveals notable differences. The α-MnO_2@C electrode exhibits a more pronounced peak intensity and a larger enclosed area in the high voltage region, which signifies greater electrochemical activity. The peaks at 1.57 and 1.6 V are distinctly visible for the α-MnO_2@C and α-MnO_2 electrodes, respectively. These observations suggest that the carbon coating has a positive effect on the electrochemical performance of α-MnO_2, enhancing its capacity and stability. Graphene, another carbon-based material, has also been used to modify MnO_2 cathodes. Wu *et al.* have demonstrated that graphene coating can play a role similar to carbon coating. It can increase the capacity of the battery cathode material and contribute to its stability[118]. The performance of the cathode material after surface engineering modification, as shown in Figure 11B and C, is superior to that of other AZIB cathode materials. This indicates that graphene coating is a valid strategy for enhancing the electrochemical properties of MnO_2 cathodes, leading to improved battery performance.

Conductive polymers, for instance, polyaniline (PANI)[119], polypyrrole[120], and polythiophene[121], are excellent candidates for coating materials in battery technology due to their high conductivity and ability to prevent the dissolution of active substances in cathode materials. The application of this coating has the potential to significantly enhance battery performance by increasing the stability of the cathode material[122]. Bao *et al.* have synthesized PANI@MnO_2 composite materials and compared the stability of α-MnO_2 and PANI@MnO_2 electrodes in a 1 mol/L Na_2SO_4 aqueous solution, as illustrated in Figure 11D and E[123]. After

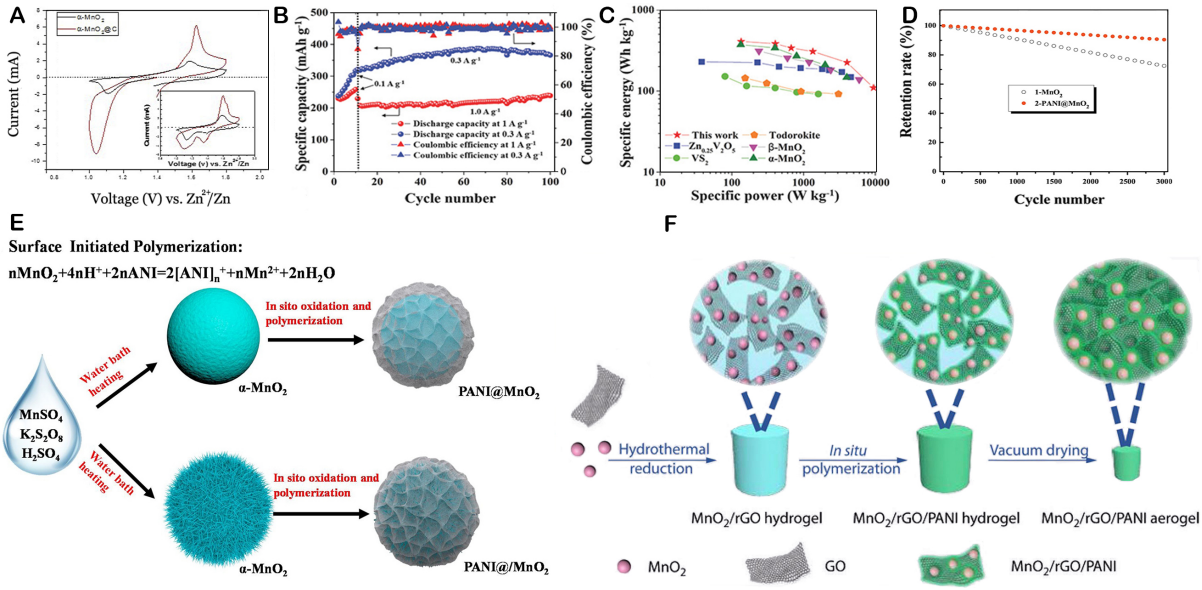

Figure 11. (A) First cycle and (inset) second cycle. This figure is reprinted (adapted) with permission from Islam *et al.* Copyright (2017) Elsevier[117]. (B) Cycling performances of MGS; (C) the Ragone plot (based on the weight of cathode material) of the MGS cell; This figure is reprinted (adapted) with permission from Wu *et al.* Copyright (2018) Wiley-VCH[118]. (D) Cycling stability of MnO_2 and PANI@MnO_2 electrodes after 3000cycles; (E) Scheme of the synthetic procedure for PANI@MnO_2 composite; (F) Schematic illustration of the preparation process of MnO_2/rGO/PANI. This figure is reprinted (adapted) with permission from Mao *et al.* Copyright (2019) Springer[122].

3,000 cycles, the α-MnO_2 electrode retained 75% of its specific capacitance, while the PANI@MnO_2 composite exhibited a higher retention rate of 90%. The enhanced stability of the PANI@MnO_2 composite is indeed due to the strong molecular interactions between the amine groups of PANI and the hydroxyl groups of MnO_2. These interactions, along with the uniform coating of PANI on the surface of MnO_2, are crucial for the electrochemical stability of the composite material. The uniform coating of PANI on MnO_2, together with the robust molecular interactions between the amine groups of PANI and the hydroxyl groups of MnO_2, contributes to the enhanced stability of the composite material[119]. This coating effectively inhibits the dissolution of MnO_2 and the degradation of PANI, leading to superior cycling stability when compared to the individual components.

Surface engineering has proven to be a powerful tool in exploiting advanced composite materials for energy storage applications. By carefully designing the surface composition and structure, it is possible to achieve a synergistic effect that enhances the performance of the material. In the case of Mn-based electrodes, surface engineering can address the issue of manganese dissolution and improve electrical conductivity. Mao *et al.* have demonstrated this concept with the development of a composite aerogel electrode material (MnO_2/rGO/PANI) [Figure 11F][122]. This material is prepared by coating PANI onto manganese dioxide (MnO_2) and then combined with reduced graphene oxide (rGO). The resulting composite, when used in a (MnO_2/rGO/PANI)/Zn battery, demonstrates a substantial capacity of 241.1 mAh g^{-1} and maintains 82.7% of its initial capacity after 600 cycles. The MnO_2/rGO aerogel has a compact and dense structure, with MnO_2 spheres encapsulated by rGO nanosheets and evenly dispersed throughout the graphene network. The N 1s spectrum, with its three distinct peaks at 399.5, 400.4 and 401.1 eV, indicates the presence of amine groups, polarons, and positively charged nitrogen species, respectively. These groups are essential for the conductivity of PANI, as they facilitate electron transfer within the polymer. The presence of these groups in the composite material suggests that the PANI coating significantly enhances the conductivity of the MnO_2/rGO aerogel[124-126]. The method offers a practical approach to overcoming the limited conductivity of

MnO_2. Kamenskii *et al.* have engineered a composite material by integrating poly(3,4-ethylenedioxythiophene):poly(styrenesulfonate) (PEDOT:PSS) into the MnO_2 framework[127]. This composite material, when used to coat MnO_2, results in a denser and smoother surface, particularly for the MnO_2/PEDOT:PSS electrode, compared to the bare MnO_2 electrode. The modification of PEDOT:PSS not only expands the surface area but also boosts the conductivity of the electrode, which makes it easier for the charge to be transported on the electrode surface. This results in a notable improvement in the capacity of the electrode and its ability to maintain its performance over multiple cycles. The MnO_2/PEDOT electrode demonstrates a remarkable specific capacity of 238 mAh g^{-1}, with an impressive capacity retention rate of 99%. In contrast, the pristine δ-MnO_2 cathode experiences a 10% decrease in capacity, whereas the modified electrodes show no capacity fading after stabilization. The structure stability is enhanced by the composite structure produced by combining organic compounds with manganese dioxide, making it more resistant to structural collapse and reducing adverse electrochemical performance caused by phase change[122]. This has been confirmed by the scanning electron microscopy (SEM) and *ex-situ* XPS analysis. Simultaneously, it improves the interaction between components. These advantages make such composite materials widely applicable in electrochemical energy storage devices such as ZIBs.

Electrolyte regulation

Electrolyte regulation is one of the most efficient methods to reduce the dissolution of cathode materials during cycling, and it plays an important role in solving the anode reversibility problem[128]. Using a $ZnSO_4$ aqueous solution as the electrolyte in AZIBs is indeed common due to its favorable electrochemical properties[129]. However, it is important to recognize that cells utilizing $ZnSO_4$ electrolytes often require an extended activation period to reach their maximum specific capacity. Furthermore, the cycling stability of AZIBs with $ZnSO_4$ electrolytes can be suboptimal [Figure 12A][130]. Therefore, strategies from the angle of electrolytes are adopted, such as replacing $ZnSO_4$ electrolytes with $Zn(CF_3SO_3)_2$, synthesizing new zinc electrolytes, and employing additives. However, so far, little has been done on new zinc salts for MnO_2 cathodes.

Adding additives can effectively inhibit Mn^{2+} dissolution, regulate the ion distribution to obtain a dendrite-free Zn anode, stabilize the electrode/electrolyte interface, and improve the adaptability to extreme environmental conditions[131]. Regulating the electrolyte composition can effectively modulate the redox potential and mitigate side reactions, thereby controlling the formation of undesirable by-products. Treating the dissolution of the cathode material as a reversible process, one can leverage Le Chatelier's principle to optimize the salt concentration of the electrolyte. This strategy aims to increase the concentration of specific cations within the electrolyte, thus declining the dissolution of these cations from the cathode material[132]. It has been particularly effective in the context of Mn-based cathode materials. Pan *et al.* have conducted research on the MnO_2/Zn battery using a mild $ZnSO_4$ electrolyte, where they observed an initial specific capacity of 210 and 255 mA h/g at 0.2 C in the first two cycles. However, they noted a rapid decrease in capacity after these initial cycles[65]. To mitigate this issue, they introduced $MnSO_4$ into the $ZnSO_4$ electrolyte, which effectively reduced the dissolution of α-MnO_2 by altering the dissolution equilibrium of Mn^{2+} from the α-MnO_2 electrodes. The CV curves in Figure 12B and C demonstrate that adding $MnSO_4$ did not disrupt the redox reaction of the MnO_2 electrode. Instead, it significantly improved the utilization rate of the MnO_2 active materials. The capacity of the electrodes was significantly improved, reaching 285 mAh g^{-1} at a C/3 rate and 260 mAh g^{-1} at a 1C rate. Furthermore, the addition of $MnSO_4$ to the electrolyte of MnO_2/Zn batteries has been found to notably enhance their long-term cycling stability. These batteries maintained an impressive capacity retention of 92% after 5,000 cycles at a demanding 5C current rate. Employing this technique on various cathode materials, including NaV_3O_8, $C_{12}Fe_2N_{12}Zn_3$, and Co_3O_4, can lead to comparable enhancements in performance. Employing high-concentration electrolytes (HCEs) is a proven method to reduce cathode dissolution, primarily due to the limited availability of free water

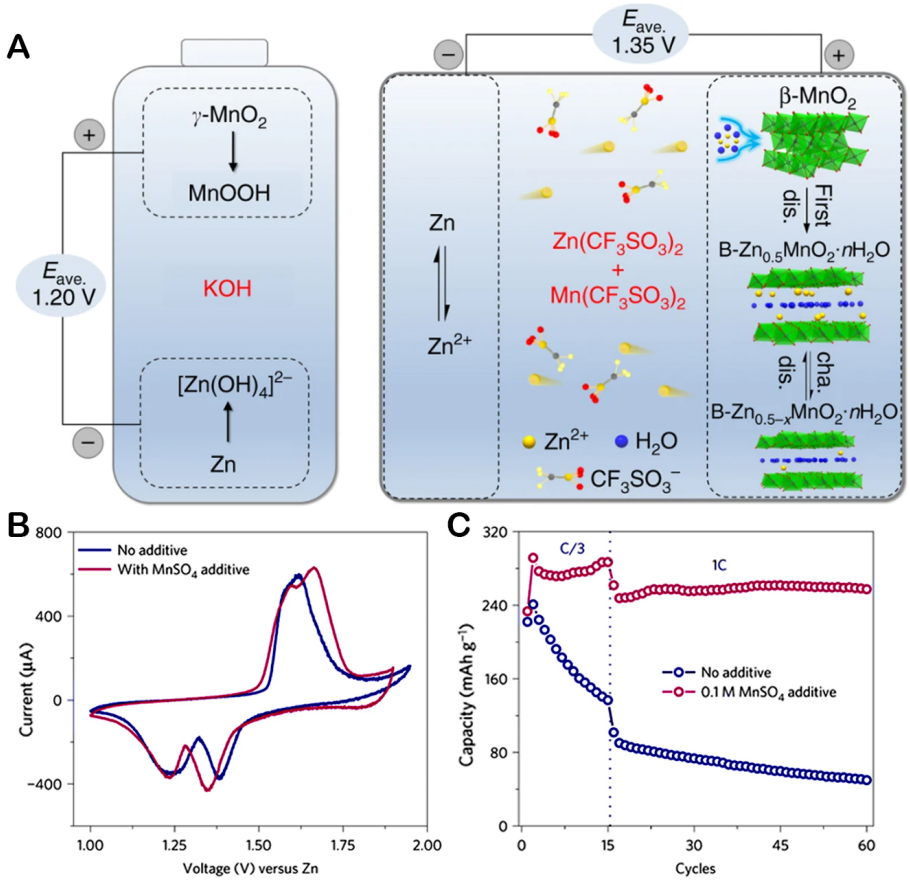

Figure 12. (A) MnO_2/Zn battery chemistry. This figure is reprinted (adapted) with permission from Zhang *et al.* Copyright (2017) Springer Science and Business Media LLC[130]. (B) CV scanning performance of MnO_2 electrodes with and without 0.1 M $MnSO_4$ additive in 2 M $ZnSO_4$ aqueous electrolyte. (C) Rate performance (using an electrolyte with a $MnSO_4$ additive). This figure is reprinted (adapted) with permission from Pan *et al.* Copyright (2016) Nature Research[65].

molecules that can be saturated within the electrolyte solution[133,134]. This strategy has been shown to be particularly effective in preventing the leaching of cations from cathode materials such as V_2O_5 and Mn_2O_3 when $ZnCl_2$-based HCEs are utilized. Using HCEs can significantly enhance the stability and longevity of these materials in battery applications[135,136]. Zhang *et al.* discovered that a $Zn(CF_3SO_3)_2$ electrolyte with additional $Mn(CF_3SO_3)_2$ performs better in inhibiting Mn2+ dissolution than a $ZnSO_4$ electrolyte with $MnSO_4$[130].

Gel electrolytes have been greatly developed for flexible AZIBs[137], which enhances the excellent cycle durability of batteries[138-140]. Further, the incorporation of solid or gel-based electrolytes in battery technology has been demonstrated to mitigate the formation of Zn dendrites[141,142]. Solid or gel electrolytes, characterized by a reduced water content and a strong adsorption affinity, can effectively prevent the manganese dissolution, contributing to achieving long-term cyclability[138].

Based on the above, the mainstream approaches to boosting the performance of MnO_2-based cathode materials have been systematically summarized [Table 4]. A primary method to achieve enhancement involves amalgamating MnO_2 into nanocomposite materials, which capitalizes on the synergistic effects of the various components to yield outstanding electrochemical performance. Elaboration on the crystal structure of MnO_2 itself, such as augmenting defect density and refining the nanostructure, can result in the

Table 4. Summary of the mainstream approaches to boosting the performance of MnO_2-cathode materials

Cathode material	Approaches	Performance (mAh g^{-1})	References
α-MnO_2 (surface area 208 m^2/g)	Nanostructure design	234 (100 mA g^{-1})	[47]
MnO_2 (surface area 153 m^2/g)	Nanostructure design	323 (16 mA g^{-1})	[100]
cw-MnO_2	Interlayer adjustment	350 (100 mA g^{-1})	[101]
A-MnO_2-δ	Nanostructure defect	301 (100 mA g^{-1})	[113]
MnO_2@Co_9S_8	Heteroatom doping	963 mF cm^{-2} (1.5 mA cm^{-2})	[115]
α-MnO_2@C	Surface modification	272 (66 mA g^{-1})	[117]
MnO_2/rGO/PANI	Surface modification	241 (100 mA g^{-1})	[122]
β-MnO_2 (aqueous $Zn(CF_3SO_3)_2$ electrolyte)	Electrolyte Regulation	275 (0.65 C)	[130]

stabilized crystal structure with enlarged interlayer spacing and the amplified surface area with more active sites. Also, surface modifications can effectuate alterations in the surface properties of MnO_2 and further speed up the kinetics of the electrochemical reaction. Further, regulating the solvent in the electrolyte, salt ratio and concentration and incorporating additives can not only enhance electrochemical performance but alter the reaction routes.

OUTLOOKS AND PERSPECTIVES

As next-generation energy storage devices, AZIBs have recently shown a lot of promise because of their low cost, excellent electrochemical performance, low toxicity, ease of production, and outstanding environmental protection. However, there are still important concerns that need to be resolved before AZIBs may be put into practice. The potential of MnO_2 cathode materials is being investigated, and research on the charge storage mechanism of MnO_2 cathodes is being actively discussed. Meanwhile, large-scale production of MnO_2-based nanocomposite electrode materials remains immature. Founded on the above discussion on the charge storage mechanism and optimization strategies for MnO_2 cathodes, we here provide an outlook on the future research directions of AZIBs [Figure 13].

(1) It is complex and debatable to the charge storage mechanism of the MnO_2 cathode. Advanced *in situ* technologies, such as electrochemical quartz crystal microbalance (EQCM), are needed to provide a more comprehensive supplement to the microelectrochemical reaction mechanism. More than *in situ* and in operando characterization, similar diffraction features among the possible Mn-based products during charging/discharging may further disturb the analysis. Hence, the electrolyte system design may play a dispensable role in analyzing the charge storage mechanism of MnO_2.

(2) The manganese dissolution-deposition in the process of charge/discharge deserve more intense attention, which is intimately related to the capacity decay of Mn-based electrodes. Importantly, it might become the key to improving the AZIB performance. To comprehensively understand its reaction paths, advanced analytical techniques, such as *in situ* spectroscopy and microscopy, can be employed to monitor its dissolution and deposition. Computational modeling and simulation can assist in predicting manganese behavior and identifying factors contributing to capacity decay. By integrating experimental and theoretical approaches, the fine details of dissolution-deposition mechanism can be explored, paving way on designing new-type Mn-based rechargeable batteries.

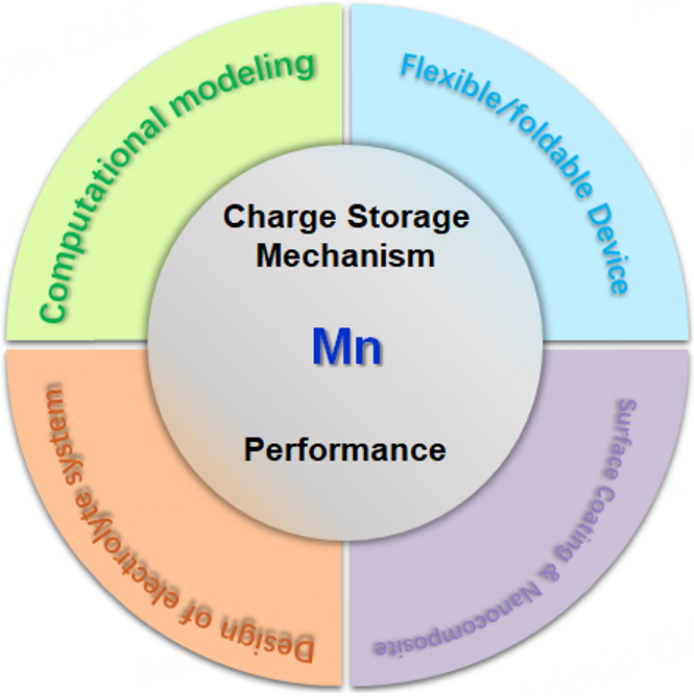

Figure 13. Outlooks on Mn-based cathodes for advancing AZIBs.

(3) Although numerous optimization strategies have been developed to modify the MnO_2 cathode material, a single strategy cannot address multiple problems simultaneously. Surface coating to form nanocomposite structure may offer the most efficient solution by integrating multi-functions to depress manganese dissolution and improve the conductivity. On the other hand, optimization strategies need to be developed with the associated charge storage mechanism. Considering this, electrolytes, which provide large room to improve the battery performance, indeed call for the scrutinization on their related charge storage mechanism, especially for emerging water-in-salt electrolytes, deep eutectic solvents, and quasi-/solid state electrolytes. Moreover, few studies remain on the effects of fluid collectors and adhesives, which are crucial for enhancing the overall performance of AZIBs[116,143-145].

(4) The subject of flexible energy storage is continuing to expand as wearable flexible electronics, health monitors, and flexible display devices gradually evolve. High-toughness, low-cost expandable ZIBs have been produced quickly. The mechanical strength, water content of gel, and the tightness of the electrolyte-to-electrode contact interface, however, may cause the battery to distort and raise its risk factor during this process. Therefore, solving these problems has become the key to developing AZIBs.

(5) Exploring advanced cathode materials and understanding charge storage mechanisms are crucial for advancing zinc battery technology. Nevertheless, lacking comprehensive engineering insights can impede the practical application of scholarly breakthroughs within industrial settings. Consequently, it is imperative to focus on assessing novel research outcomes against critical benchmarks. This approach will expedite the shift from theoretical research to the widespread implementation of energy storage systems within real-world power networks and manufacturing processes. The critical benchmarks encompass energy storage capacity, safety, cost-effectiveness, the anode-to-cathode capacity ratio, *etc*.

Despite the significant achievements for the long-being explored MnO_2 cathode materials, critical issues persist, necessitating further research to realize their application for AZIBs. In view of this, we comprehensively summarize the charge storage mechanisms for these materials in AZIBs, with current concern on the pH-dependent process and time-evolving trend. The main challenges and equivalent optimization strategies to MnO_2 cathodes are then presented and analyzed thoroughly. With the above discussion, outlooks are provided from the perspectives of charge storage mechanism, advanced material/electrode design, and interdisciplinary functional design. We envision this review provide an insightful guide on the future development of advancing Mn-based AZIBs.

DECLARATIONS

Authors' contributions

Substantial contributions to conception and design of the study, and project administration: Dai C, Yao M, Yuan D

Assistance in the design of the study, manuscript editing, and administrative support: Wang Q, Cai W, Zhang Y

Manuscript drafting and editing and technical support: Luo C, Lei H, Xiao Y, Nie X, Li Y

Availability of data and materials

Not applicable.

Financial support and sponsorship

This work was financially supported by the National Key Research and Development Program (2021YFB2400202), the Fundamental Research Funds for the Central Universities (No. YJ202280), the 100 Talented Team of Hunan Province (XiangZu [2016] 91), and the Natural Science Foundation of Hunan Province (2022JJ30613).

Conflicts of interest

All authors declared that there are no conflicts of interest.

Ethical approval and consent to participate

Not applicable.

Consent for publication

Not applicable.

REFERENCES

1. Jing J, Liu M, Colvin VL, Li W, Yu WW. Photocatalytic degradation of nitrogen-containing organic compounds over TiO_2. *J Mol Catal A Chem* 2011;351:17-28. DOI
2. Guan P, Zhou L, Yu Z, et al. Recent progress of surface coating on cathode materials for high-performance lithium-ion batteries. *J Energy Chem* 2020;43:220-35. DOI
3. Ponrouch A, Frontera C, Bardé F, Palacín MR. Towards a calcium-based rechargeable battery. *Nat Mater* 2016;15:169-72. DOI PubMed
4. Nam KW, Kim S, Lee S, et al. The high performance of crystal water containing manganese birnessite cathodes for magnesium batteries. *Nano Lett* 2015;15:4071-9. DOI
5. Saha P, Datta MK, Velikokhatnyi OI, Manivannan A, Alman D, Kumta PN. Rechargeable magnesium battery: current status and key challenges for the future. *Prog Mater Sci* 2014;66:1-86. DOI
6. Muldoon J, Bucur CB, Oliver AG, et al. Electrolyte roadblocks to a magnesium rechargeable battery. *Energy Environ Sci*

2012;5:5941-50. DOI
7. Pramudita JC, Sehrawat D, Goonetilleke D, Sharma N. An initial review of the status of electrode materials for potassium-ion batteries. *Adv Energy Mater* 2017;7:1602911. DOI
8. Han J, Niu Y, Bao SJ, Yu YN, Lu SY, Xu M. Nanocubic $KTi_2(PO_4)_3$ electrodes for potassium-ion batteries. *Chem Commun* 2016;52:11661-4. DOI
9. Jian Z, Luo W, Ji X. Carbon electrodes for K-ion batteries. *J Am Chem Soc* 2015;137:11566-9. DOI PubMed
10. Hueso KB, Armand M, Rojo T. High temperature sodium batteries: status, challenges and future trends. *Energy Environ Sci* 2013;6:734-49. DOI
11. Luo C, Xu Y, Zhu Y, et al. Selenium@mesoporous carbon composite with superior lithium and sodium storage capacity. *ACS Nano* 2013;7:8003-10. DOI
12. Yang X, Xu J, Chang Z, et al. Blood-capillary-inspired, free-standing, flexible, and low-cost super-hydrophobic N-CNTs@SS cathodes for high-capacity, high-rate, and stable Li-air batteries. *Adv Energy Mater* 2018;8:1702242. DOI
13. Abouimrane A, Dambournet D, Chapman KW, Chupas PJ, Weng W, Amine K. A new class of lithium and sodium rechargeable batteries based on selenium and selenium-sulfur as a positive electrode. *J Am Chem Soc* 2012;134:4505-8. DOI PubMed
14. Liu J, Xu C, Chen Z, Ni S, Shen ZX. Progress in aqueous rechargeable batteries. *Green Energy Environ* 2018;3:20-41. DOI
15. Wang Q, Sarkar A, Wang D, et al. Multi-anionic and -cationic compounds: new high entropy materials for advanced Li-ion batteries. *Energy Environ Sci* 2019;12:2433-42. DOI
16. Wang Q, Yao M, Zhu A, Wang Q, Wu H, Zhang Y. Semi-metallic superionic layers suppressing voltage fading of Li-rich layered oxide towards superior-stable Li-ion batteries. *Angew Chem Int Ed* 2023;62:e202309049. DOI
17. Kang S, Cheng J, Gao W, Cui L. Toward safer lithium metal batteries: a review. *Energy Mater* 2023;3:300043. DOI
18. Pan Z, Liu X, Yang J, et al. Aqueous rechargeable multivalent metal-ion batteries: advances and challenges. *Adv Energy Mater* 2021;11:2100608. DOI
19. Qiu S, Xu Y, Wu X, Ji X. Prussian blue analogues as electrodes for aqueous monovalent ion batteries. *Electrochem Energy Rev* 2022;5:242-62. DOI
20. Dong N, Zhang F, Pan H. Towards the practical application of Zn metal anodes for mild aqueous rechargeable Zn batteries. *Chem Sci* 2022;13:8243-52. DOI PubMed PMC
21. Wan F, Zhang Y, Zhang L, et al. Reversible Oxygen redox chemistry in aqueous zinc-ion batteries. *Angew Chem Int Ed* 2019;58:7062-7. DOI
22. Zhao K, Wang C, Yu Y, et al. Ultrathin surface coating enables stabilized zinc metal anode. *Adv Mater Inter* 2018;5:1800848. DOI
23. Yang F, Yuwono JA, Hao J, et al. Understanding H_2 evolution electrochemistry to minimize solvated water impact on zinc-anode performance. *Adv Mater* 2022;34:e2206754. DOI
24. Zhao G, Rui K, Dou SX, Sun W. Heterostructures for electrochemical hydrogen evolution reaction: a review. *Adv Funct Mater* 2018;28:1803291. DOI
25. Wang F, Borodin O, Gao T, et al. Highly reversible zinc metal anode for aqueous batteries. *Nat Mater* 2018;17:543-9. DOI
26. Kim JY, Liu G, Shim GY, Kim H, Lee JK. Functionalized Zn@ZnO hexagonal pyramid array for dendrite-free and ultrastable zinc metal anodes. *Adv Funct Mater* 2020;30:2004210. DOI
27. He H, Tong H, Song X, Song X, Liu J. Highly stable Zn metal anodes enabled by atomic layer deposited Al_2O_3 coating for aqueous zinc-ion batteries. *J Mater Chem A* 2020;8:7836-46. DOI
28. Tarascon JM, Armand M. Issues and challenges facing rechargeable lithium batteries. *Nature* 2001;414:359-67. DOI PubMed
29. Olivetti EA, Ceder G, Gaustad GG, Fu X. Lithium-ion battery supply chain considerations: analysis of potential bottlenecks in critical metals. *Joule* 2017;1:229-43. DOI
30. Wang L, Wang P, Wang T, Yin Y, Guo Y, Wang C. Prussian blue nanocubes as cathode materials for aqueous Na-Zn hybrid batteries. *J Power Sources* 2017;355:18-22. DOI
31. Liu X, Ma L, Du Y, Lu Q, Yang A, Wang X. Vanadium pentoxide nanofibers/carbon nanotubes hybrid film for high-performance aqueous zinc-ion batteries. *Nanomaterials* 2021;11:1054. DOI PubMed PMC
32. Li Y, Yu D, Lin S, Sun D, Lei Z. Preparation of α-MnO_2 nanorods/porous carbon cathode for aqueous zinc-ion batteries. *Acta Chimica Sinica* 2021;79:200-7. DOI
33. Li Z, Liu T, Meng R, et al. Insights into the structure stability of prussian blue for aqueous zinc ion batteries. *Energy Environ Mater* 2021;4:111-6. DOI
34. Liu Q, Ma Z, Chen Z, et al. A polyaniline surface-modified Prussian blue analogue cathode for flexible aqueous Zn-ion batteries. *Chem Commun* 2022;58:8226-9. DOI
35. Sun W, Wang F, Hou S, et al. Zn/MnO_2 battery chemistry with H^+ and Zn^{2+} coinsertion. *J Am Chem Soc* 2017;139:9775-8. DOI
36. Wu P, Kong X, Feng Y, et al. Phase engineering on amorphous/crystalline γ-Fe_2O_3 nanosheets for boosting dielectric loss and high-performance microwave absorption. *Adv Funct Mater* 2024;34:2311983. DOI
37. Ding J, Du Z, Li B, et al. Unlocking the potential of disordered rocksalts for aqueous zinc-ion batteries. *Adv Mater* 2019;31:e1904369. DOI
38. Caldeira V, Rouget R, Fourgeot F, et al. Controlling the shape change and dendritic growth in Zn negative electrodes for application in Zn/Ni batteries. *J Power Sources* 2017;350:109-16. DOI
39. Wang X, Wang F, Wang L, et al. An aqueous rechargeable Zn//Co_3O_4 Battery with high energy density and good cycling behavior.

Adv Mater 2016;28:4904-11. DOI
40. Zhou J, Shan L, Wu Z, Guo X, Fang G, Liang S. Investigation of V_2O_5 as a low-cost rechargeable aqueous zinc ion battery cathode. *Chem Commun* 2018;54:4457-60. DOI
41. He P, Yan M, Zhang G, et al. Layered VS_2 nanosheet-based aqueous Zn ion battery cathode. *Adv Energy Mater* 2017;7:1601920. DOI
42. Jia Z, Wang B, Wang Y. Copper hexacyanoferrate with a well-defined open framework as a positive electrode for aqueous zinc ion batteries. *Mater Chem Phys* 2015;149-50:601-6. DOI
43. Zhang L, Chen L, Zhou X, Liu Z. Towards high-voltage aqueous metal-ion batteries beyond 1.5 V: the zinc/zinc hexacyanoferrate system. *Adv Energy Mater* 2015;5:1400930. DOI
44. Alfaruqi MH, Gim J, Kim S, et al. Enhanced reversible divalent zinc storage in a structurally stable α-MnO_2 nanorod electrode. *J Power Sources* 2015;288:320-7. DOI
45. Islam S, Alfaruqi MH, Mathew V, et al. Facile synthesis and the exploration of the zinc storage mechanism of β-MnO_2 nanorods with exposed (101) planes as a novel cathode material for high performance eco-friendly zinc-ion batteries. *J Mater Chem A* 2017;5:23299-309. DOI
46. Alfaruqi MH, Mathew V, Gim J, et al. Electrochemically induced structural transformation in a γ-MnO_2 cathode of a high capacity zinc-ion battery system. *Chem Mater* 2015;27:3609-20. DOI
47. Wei C, Xu C, Li B, Du H, Kang F. Preparation and characterization of manganese dioxides with nano-sized tunnel structures for zinc ion storage. *J Phys Chem Solids* 2012;73:1487-91. DOI
48. Xuan X, Qian M, Pan L, et al. A hollow tubular NiCo layacknered double hydroxide@Ag nanowire structure for high-power-density flexible aqueous Ni//Zn battery. *J Energy Chem* 2022;70:593-603. DOI
49. Huang J, Li Y, Xie R, et al. Structural engineering of cathodes for improved Zn-ion batteries. *J Energy Chem* 2021;58:147-55. DOI
50. Cui Y, Ding Y, Guo L, et al. Ultra-long $Zn_3V_2O_7(OH)_2{\cdot}2H_2O$ nanowires grown on carbon cloth as cathode material for aqueous zinc-ion batteries. *Energy Mater* 2023;3:300023. DOI
51. Zhu Y, Guan P, Zhu R, et al. Recent advances in flexible alkaline zinc-based batteries: materials, structures, and perspectives. *J Energy Chem* 2023;87:61-88. DOI
52. Lu C, Yang Z, Wang Y, et al. Ethylene glycol-regulated ammonium vanadate with stable layered structure and favorable interplanar spacing as high-performance cathode for aqueous zinc ion batteries. *Chin Chem Lett* 2023;34:108572. DOI
53. Wei W, Cui X, Chen W, Ivey DG. Manganese oxide-based materials as electrochemical supercapacitor electrodes. *Chem Soc Rev* 2011;40:1697-721. DOI PubMed
54. Gao X, Wu H, Li W, et al. H^+-insertion boosted α-MnO_2 for an aqueous Zn-ion battery. *Small* 2020;16:e1905842. DOI
55. Wan F, Zhang L, Dai X, Wang X, Niu Z, Chen J. Aqueous rechargeable zinc/sodium vanadate batteries with enhanced performance from simultaneous insertion of dual carriers. *Nat Commun* 2018;9:1656. DOI PubMed PMC
56. Álvarez-serrano I, Almodóvar P, Giraldo DA, Llopis F, Solsona B, López ML. Stable manganese-oxide composites as cathodes for Zn-ion batteries: interface activation from in situ layer electrochemical deposition under 2 V. *Adv Mater Inter* 2022;9:2101924. DOI
57. Shen Z, Tang Z, Li C, et al. Precise proton redistribution for two-electron redox in aqueous zinc/manganese dioxide batteries. *Adv Energy Mater* 2021;11:2102055. DOI
58. Jing F, Liu Y, Shang Y, et al. Dual ions intercalation drives high-performance aqueous Zn-ion storage on birnessite-type manganese oxides cathode. *Energy Stor Mater* 2022;49:164-71. DOI
59. Zhao Y, Zhang P, Liang J, et al. Unlocking layered double hydroxide as a high-performance cathode material for aqueous zinc-ion batteries. *Adv Mater* 2022;34:e2204320. DOI
60. Guo D, Zhao W, Pan F, Liu G. Block copolymer-derived porous carbon fibers enable high MnO_2 loading and fast charging in aqueous zinc-ion battery. *Batteries Supercaps* 2022;5:e202100380. DOI
61. Dai H, Zhou R, Zhang Z, Zhou J, Sun G. Design of manganese dioxide for supercapacitors and zinc-ion batteries: similarities and differences. *Energy Mater* 2022;2:200040. DOI
62. Chen H, Dai C, Xiao F, et al. Reunderstanding the reaction mechanism of aqueous Zn-Mn batteries with sulfate electrolytes: role of the zinc sulfate hydroxide. *Adv Mater* 2022;34:e2109092. DOI
63. Shoji T, Hishinuma M, Yamamoto T. Zinc-manganese dioxide galvanic cell using zinc sulphate as electrolyte. Rechargeability of the cell. *J Appl Electrochem* 1988;18:521-6. DOI
64. Xu C, Li B, Du H, Kang F. Energetic zinc ion chemistry: the rechargeable zinc ion battery. *Angew Chem Int Ed* 2012;51:933-5. DOI PubMed
65. Pan H, Shao Y, Yan P, et al. Reversible aqueous zinc/manganese oxide energy storage from conversion reactions. *Nat Energy* 2016;1:16039. DOI
66. Zhu C, Fang G, Liang S, et al. Electrochemically induced cationic defect in MnO intercalation cathode for aqueous zinc-ion battery. *Energy Stor Mater* 2020;24:394-401. DOI
67. Khamsanga S, Pornprasertsuk R, Yonezawa T, Mohamad AA, Kheawhom S. δ-MnO_2 nanoflower/graphite cathode for rechargeable aqueous zinc ion batteries. *Sci Rep* 2019;9:8441. DOI PubMed PMC
68. Alfaruqi MH, Gim J, Kim S, et al. A layered δ-MnO_2 nanoflake cathode with high zinc-storage capacities for eco-friendly battery applications. *Electrochem Commun* 2015;60:121-5. DOI
69. Mathew V, Sambandam B, Kim S, et al. Manganese and vanadium oxide cathodes for aqueous rechargeable zinc-ion batteries: a

focused view on performance, mechanism, and developments. *ACS Energy Lett* 2020;5:2376-400. DOI

70. Fu Y, Wei Q, Zhang G, et al. High-performance reversible aqueous Zn-ion battery based on porous MnO_x nanorods coated by MOF-derived N-doped carbon. *Adv Energy Mater* 2018;8:1801445. DOI
71. Wang Q, Liu Y, Chen P. Phenazine-based organic cathode for aqueous zinc secondary batteries. *J Power Sources* 2020;468:228401. DOI
72. Huang Y, Mou J, Liu W, et al. Novel insights into energy storage mechanism of aqueous rechargeable Zn/MnO_2 batteries with participation of Mn_2. *Nanomicro Lett* 2019;11:49. DOI PubMed PMC
73. Zhao Q, Chen X, Wang Z, et al. Unravelling H^+/Zn^{2+} synergistic intercalation in a novel phase of manganese oxide for high-performance aqueous rechargeable battery. *Small* 2019;15:e1904545. DOI
74. Wang L, Zheng J. Recent advances in cathode materials of rechargeable aqueous zinc-ion batteries. *Mater Today Adv* 2020;7:100078. DOI
75. Qiu N, Chen H, Yang Z, Sun S, Wang Y. Synthesis of manganese-based complex as cathode material for aqueous rechargeable batteries. *RSC Adv* 2018;8:15703-8. DOI PubMed PMC
76. Siamionau U, Aniskevich Y, Mazanik A, et al. Rechargeable zinc-ion batteries with manganese dioxide cathode: How critical is choice of manganese dioxide polymorphs in aqueous solutions? *J Power Sources* 2022;523:231023. DOI
77. Bi S, Wu Y, Cao A, Tian J, Zhang S, Niu Z. Free-standing three-dimensional carbon nanotubes/amorphous MnO_2 cathodes for aqueous zinc-ion batteries with superior rate performance. *Mater Today Energy* 2020;18:100548. DOI
78. Liu W, Zhang X, Huang Y, et al. β-MnO_2 with proton conversion mechanism in rechargeable zinc ion battery. *J Energy Chem* 2021;56:365-73. DOI
79. Kang J, Zhao Z, Li H, Meng Y, Hu B, Lu H. An overview of aqueous zinc-ion batteries based on conversion-type cathodes. *Energy Mater* 2022;2:200009. DOI
80. Xu Y, Huang W, Liu J, et al. Promoting the reversibility of electrolytic MnO_2-Zn battery with high areal capacity by $VOSO_4$ mediator. *Energy Mater* 2024;4:400005. DOI
81. Liang G, Mo F, Li H, et al. A universal principle to design reversible aqueous batteries based on deposition-dissolution mechanism. *Adv Energy Mater* 2019;9:1901838. DOI
82. Guo X, Zhou J, Bai C, Li X, Fang G, Liang S. Zn/MnO_2 battery chemistry with dissolution-deposition mechanism. *Mater Today Energy* 2020;16:100396. DOI
83. Kankanallu VR, Zheng X, Leschev D, et al. Elucidating a dissolution-deposition reaction mechanism by multimodal synchrotron X-ray characterization in aqueous Zn/MnO_2 batteries. *Energy Environ Sci* 2023;16:2464-82. DOI
84. Li H, Yao H, Sun X, et al. Interface regulated MnO_2/Mn^{2+} redox chemistry in aqueous Zn ion batteries. *Chem Eng J* 2022;446:137205. DOI
85. Lee B, Seo HR, Lee HR, et al. Critical role of pH evolution of electrolyte in the reaction mechanism for rechargeable zinc batteries. *ChemSusChem* 2016;9:2948-56. DOI
86. Wang L, Cao X, Xu L, Chen J, Zheng J. Transformed akhtenskite MnO_2 from Mn_3O_4 as cathode for a rechargeable aqueous zinc ion battery. *ACS Sustain Chem Eng* 2018;6:16055-63. DOI
87. Kim SH, Oh SM. Degradation mechanism of layered MnO_2 cathodes in Zn/$ZnSO_4$/MnO_2 rechargeable cells. *J Power Sources* 1998;72:150-8. DOI
88. Yang H, Zhang T, Chen D, et al. Protocol in evaluating capacity of Zn-Mn aqueous batteries: a clue of pH. *Adv Mater* 2023;35:e2300053. DOI
89. Sambandam B, Mathew V, Kim S, et al. An analysis of the electrochemical mechanism of manganese oxides in aqueous zinc batteries. *Chem* 2022;8:924-46. DOI
90. Ma Y, Xu M, Liu R, et al. Molecular tailoring of MnO_2 by bismuth doping to achieve aqueous zinc-ion battery with capacitor-level durability. *Energy Stor Mater* 2022;48:212-22. DOI
91. Wang C, Zeng Y, Xiao X, et al. γ-MnO_2 nanorods/graphene composite as efficient cathode for advanced rechargeable aqueous zinc-ion battery. *J Energy Chem* 2020;43:182-7. DOI
92. Zhao M, Luo Y, Zhu L, et al. Ultrathin δ-MnO_2 nanosheets branched onto N-doped carbon nanotubes as binder-free cathode electrodes for aqueous zinc-ion batteries with a high areal capacity. *J Alloys Compd* 2022;913:165124. DOI
93. Li L, Yang Q, Wang D, et al. Facile synthesis λ-MnO_2 spinel for highly effective catalytic oxidation of benzene. *Chem Eng J* 2021;421:127828. DOI
94. Zhang N, Cheng F, Liu Y, et al. Cation-deficient spinel $ZnMn_2O_4$ cathode in $Zn(CF_3SO_3)_2$ electrolyte for rechargeable aqueous zn-ion battery. *J Am Chem Soc* 2016;138:12894-901. DOI
95. Pam ME, Yan D, Yu J, et al. Microstructural engineering of cathode materials for advanced zinc-ion aqueous batteries. *Adv Sci* 2020;8:2002722. DOI PubMed PMC
96. Yu Z, Tetard L, Zhai L, Thomas J. Supercapacitor electrode materials: nanostructures from 0 to 3 dimensions. *Energy Environ Sci* 2015;8:702-30. DOI
97. Hao J, Mou J, Zhang J, et al. Electrochemically induced spinel-layered phase transition of Mn_3O_4 in high performance neutral aqueous rechargeable zinc battery. *Electrochim Acta* 2018;259:170-8. DOI
98. Wang Y, Li H, He P, Hosono E, Zhou H. Nano active materials for lithium-ion batteries. *Nanoscale* 2010;2:1294-305. DOI
99. Song H, Liu Y, Zhang C, Liu C, Cao G. Mo-doped LiV_3O_8 nanorod-assembled nanosheets as a high performance cathode material for

lithium ion batteries. *J Mater Chem A* 2015;3:3547-58. DOI

100. Alfaruqi MH, Islam S, Gim J, et al. A high surface area tunnel-type α-MnO_2 nanorod cathode by a simple solvent-free synthesis for rechargeable aqueous zinc-ion batteries. *Chem Phys Lett* 2016;650:64-8. DOI
101. Nam KW, Kim H, Choi JH, Choi JW. Crystal water for high performance layered manganese oxide cathodes in aqueous rechargeable zinc batteries. *Energy Environ Sci* 2019;12:1999-2009. DOI
102. Li X, Zhou Q, Yang Z, et al. Unraveling the role of nitrogen-doped carbon nanowires incorporated with MnO_2 nanosheets as high performance cathode for zinc-ion batteries. *Energy Environ Mater* 2023;6:e12378. DOI
103. Zhang Y, Deng S, Li Y, et al. Anchoring MnO_2 on nitrogen-doped porous carbon nanosheets as flexible arrays cathodes for advanced rechargeable Zn-MnO_2 batteries. *Energy Stor Mater* 2020;29:52-9. DOI
104. Liu G, Huang H, Bi R, Xiao X, Ma T, Zhang L. K^+ pre-intercalated manganese dioxide with enhanced Zn^{2+} diffusion for high rate and durable aqueous zinc-ion batteries. *J Mater Chem A* 2019;7:20806-12. DOI
105. Hong S, Jin S, Deng Y, et al. Efficient scalable hydrothermal synthesis of MnO_2 with controlled polymorphs and morphologies for enhanced battery cathodes. *ACS Energy Lett* 2023;8:1744-51. DOI
106. Wang H, Yin K, Qin N, et al. Oxygen-deficient titanium dioxide as a functional host for lithium-sulfur batteries. *J Mater Chem A* 2019;7:10346-53. DOI
107. Ren Q, Qin N, Liu B, et al. An oxygen-deficient vanadium oxide@N-doped carbon heterostructure for sodium-ion batteries: insights into the charge storage mechanism and enhanced reaction kinetics. *J Mater Chem A* 2020;8:3450-8. DOI
108. Uchaker E, Zheng YZ, Li S, Candelaria SL, Hu S, Cao GZ. Better than crystalline: amorphous vanadium oxide for sodium-ion batteries. *J Mater Chem A* 2014;2:18208-14. DOI
109. Ku JH, Ryu JH, Kim SH, Han OH, Oh SM. Reversible lithium storage with high mobility at structural defects in amorphous molybdenum dioxide electrode. *Adv Funct Mater* 2012;22:3658-64. DOI
110. Xiao D, Lv X, Fan J, Li Q, Chen Z. Zn-based batteries for energy storage. *Energy Mater* 2023;3:300007. DOI
111. Huang S, Liu L, Zheng Y, et al. Efficient sodium storage in rolled-up amorphous Si nanomembranes. *Adv Mater* 2018;30:e1706637. DOI
112. Fan L, Li X, Yan B, et al. Controlled SnO_2 crystallinity effectively dominating sodium storage performance. *Adv Energy Mater* 2016;6:1502057. DOI
113. Cai Y, Chua R, Huang S, Ren H, Srinivasan M. Amorphous manganese dioxide with the enhanced pseudocapacitive performance for aqueous rechargeable zinc-ion battery. *Chem Eng J* 2020;396:125221. DOI
114. Liang R, Fu J, Deng Y, et al. Parasitic electrodeposition in Zn-MnO_2 batteries and its suppression for prolonged cyclability. *Energy Stor Mater* 2021;36:478-84. DOI
115. Hu Q, Jiang X, He M, Zheng Q, Lam KH, Lin D. Core-shell nanostructured MnO_2@Co_9S_8 arrays for high-performance supercapacitors. *Electrochim Acta* 2020;338:135896. DOI
116. Li Q, Wang Y, Mo F, et al. Calendar life of Zn batteries based on Zn anode with Zn powder/current collector structure. *Adv Energy Mater* 2021;11:2003931. DOI
117. Islam S, Alfaruqi MH, Song J, et al. Carbon-coated manganese dioxide nanoparticles and their enhanced electrochemical properties for zinc-ion battery applications. *J Energy Chem* 2017;26:815-9. DOI
118. Wu B, Zhang G, Yan M, et al. Graphene scroll-coated α-MnO_2 nanowires as high-performance cathode materials for aqueous Zn-ion battery. *Small* 2018;14:e1703850. DOI
119. Gök A, Sarı B, Talu M. Synthesis and characterization of conducting substituted polyanilines. *Synth Met* 2004;142:41-8. DOI
120. Benhaddad L, Gamby J, Makhloufi L, Pailleret A, Pillier F, Takenouti H. Improvement of capacitive performances of symmetric carbon/carbon supercapacitors by addition of nanostructured polypyrrole powder. *J Power Sources* 2016;307:297-307. DOI
121. Lu Q, Zhou Y. Synthesis of mesoporous polythiophene/MnO_2 nanocomposite and its enhanced pseudocapacitive properties. *J Power Sources* 2011;196:4088-94. DOI
122. Mao J, Wu F, Shi W, et al. Preparation of polyaniline-coated composite aerogel of MnO_2 and reduced graphene oxide for high-performance zinc-ion battery. *Chin J Polym Sci* 2020;38:514-21. DOI
123. Bao X, Zhang Z, Zhou D. Pseudo-capacitive performance enhancement of α-MnO_2 via in situ coating with polyaniline. *Synth Met* 2020;260:116271. DOI
124. Zang X, Li X, Zhu M, et al. Graphene/polyaniline woven fabric composite films as flexible supercapacitor electrodes. *Nanoscale* 2015;7:7318-22. DOI
125. Tantawy HR, Kengne BF, Mcilroy DN, et al. X-ray photoelectron spectroscopy analysis for the chemical impact of solvent addition rate on electromagnetic shielding effectiveness of HCl-doped polyaniline nanopowders. *J Appl Phys* 2015;118:175501. DOI
126. Han J, Wang K, Liu W, et al. Rational design of nano-architecture composite hydrogel electrode towards high performance Zn-ion hybrid cell. *Nanoscale* 2018;10:13083-91. DOI
127. Kamenskii MA, Volkov FS, Eliseeva SN, Holze R, Kondratiev VV. Comparative Study of PEDOT- and PEDOT:PSS Modified δ-MnO_2 cathodes for aqueous zinc batteries with enhanced properties. *J Electrochem Soc* 2023;170:010505. DOI
128. Li Y, Yao H, Liu X, Yang X, Yuan D. Roles of electrolyte additive in Zn chemistry. *Nano Res* 2023;16:9179-94. DOI
129. Qiu N, Chen H, Yang Z, Sun S, Wang Y. Low-cost birnessite as a promising cathode for high-performance aqueous rechargeable batteries. *Electrochim Acta* 2018;272:154-60. DOI
130. Zhang N, Cheng F, Liu J, et al. Rechargeable aqueous zinc-manganese dioxide batteries with high energy and power densities. *Nat*

Commun 2017;8:405. DOI PubMed PMC
131. Fan W, Xiong X, Xu Y, et al. Constructing stable Zn anodes for aqueous rechargeable zinc batteries. *Next Energy* 2023;1:100049. DOI
132. Bhattachar SN, Deschenes LA, Wesley JA. Solubility: it's not just for physical chemists. *Drug Discov Today* 2006;11:1012-8. DOI
133. Tie Z, Niu Z. Design strategies for high-performance aqueous Zn/organic batteries. *Angew Chem Int Ed* 2020;59:21293-303. DOI PubMed
134. Tie Z, Liu L, Deng S, Zhao D, Niu Z. Proton insertion chemistry of a zinc-organic battery. *Angew Chem Int Ed* 2020;59:4920-4. DOI PubMed
135. Liu S, He J, Liu D, et al. Suppressing vanadium dissolution by modulating aqueous electrolyte structure for ultralong lifespan zinc ion batteries at low current density. *Energy Stor Mater* 2022;49:93-101. DOI
136. Liu N, Wu X, Yin Y, et al. Constructing the efficient ion diffusion pathway by introducing oxygen defects in Mn_2O_3 for high-performance aqueous zinc-ion batteries. *ACS Appl Mater Interfaces* 2020;12:28199-205. DOI
137. Jin X, Song L, Dai C, et al. A flexible aqueous zinc-iodine microbattery with unprecedented energy density. *Adv Mater* 2022;34:e2109450. DOI
138. Geng Y, Pan L, Peng Z, et al. Electrolyte additive engineering for aqueous Zn ion batteries. *Energy Stor Mater* 2022;51:733-55. DOI
139. Chen M, Zhou W, Wang A, et al. Anti-freezing flexible aqueous Zn-MnO_2 batteries working at -35 °C enabled by a borax-crosslinked polyvinyl alcohol/glycerol gel electrolyte. *J Mater Chem A* 2020;8:6828-41. DOI
140. Liu X, Li X, Yang X, et al. Influence of water on gel electrolytes for zinc-ion batteries. *Chem Asian J* 2023;18:e202201280. DOI
141. Yuan D, Li X, Yao H, et al. A liquid crystal ionomer-type electrolyte toward ordering-induced regulation for highly reversible zinc ion battery. *Adv Sci* 2023;10:e2206469. DOI PubMed PMC
142. Yuan D, Zhao J, Ren H, et al. Anion texturing towards dendrite-free Zn anode for aqueous rechargeable batteries. *Angew Chem Int Ed* 2021;60:7213-9. DOI
143. Liu B, Yuan X, Li Y. Colossal capacity loss during calendar aging of Zn battery chemistries. *ACS Energy Lett* 2023;8:3820-8. DOI
144. Zhu R, Xiong Z, Yang H, et al. Anode/cathode dual-purpose aluminum current collectors for aqueous zinc-ion batteries. *Adv Funct Mater* 2023;33:2211274. DOI
145. Mu Y, Li Z, Wu BK, et al. 3D hierarchical graphene matrices enable stable Zn anodes for aqueous Zn batteries. *Nat Commun* 2023;14:4205. DOI PubMed PMC